Choline transport links phospholipid metabolism and inflammation in macrophages

By

Shayne Snider

Thesis submitted to the

Faculty of Graduate and Postdoctoral Studies

in partial fulfillment of the requirements

for the degree of Master of Science in Biochemistry

Department of Biochemistry, Microbiology, and Immunology

Faculty of Medicine

University of Ottawa

Abstract

Choline is necessary for the synthesis of phosphatidylcholine (PC), the predominant phospholipid species and an important lipid intermediate. Macrophages, critical mediators of innate immunity, have been implicated in lipid dysregulation associated with metabolic disease. Despite the importance of choline in lipid metabolism, few studies have investigated the relationship between choline metabolism and inflammation. My research revealed that macrophage polarization increased choline metabolism and the expression of the choline transporter CTL1. In addition, choline deficient macrophages showed altered cytokine secretion, suggesting choline metabolism may play an important role in regulating the immune response. This study also describes the generation of a novel CTL1$^{-/-}$ mouse, which showed decreased choline uptake and incorporation into lipids. As an *in vivo* model for choline deficiency, CTL1$^{-/-}$ mice represent an important model for the future study of choline metabolism. Altogether, these findings suggest an important relationship exists between choline metabolism and inflammation.

Acknowledgements

First and foremost I would like to thank Dr. Morgan Fullerton for giving me the opportunity to work in his lab. Your guidance and support has made the past two years the most fulfilling academic experience of my life. You have always been approachable and insightful, even during the ups and downs that invariably come with the task of completing a graduate degree. It is hard to believe that two years ago the lab was simply an empty room. Being able to see its transformation from the ground up is an experience not many people get to experience and one I am incredibly grateful for.

I would also like to thank all of the members of the Fullerton lab who have not only helped facilitate my research by sharing knowledge and expertise but have made the past two years thoroughly enjoyable. To my fellow graduate students Nick and Rebecca, our technician Chelsea, the undergraduates Nick, Zach, Kathryn, Kaitlyn, and Leah, thank you for everything you guys have done. I would like to especially thank Kaitlyn for all the support she provided in conducting my research. You have provided considerable time and effort to assist me with my experiments and I am truly grateful.

Most importantly I would like to thank my friends and family for their unconditional love and support. You guys have always been there when I've needed you most, for which I am endlessly appreciative.

TABLE OF CONTENTS

List of abbreviations

PC	Phosphatidylcholine
CCT	Phosphocholine cytidylyltransferase
CPT	Choline phosphotransferase
DAG	Diacylglycerol
CK	Choline Kinase
PE	Phosphatidylethanolamine
PEMT	Phosphatidylethanolamine N-methyltransferase
Lyso-PC	Lysophosphatidylcholine
CHT1	High affinity choline transporter
OCT	Organic ion transporter
CTL	Choline transporter-like protein
HC-3	Hemicholinium-3
DMAE	2-dimethylaminoethanol
TNF	Tumour necrosis factor
IL-6	Interleukin-6
IL-10	Interleukin-10
IL-1β	Interleukin-1β
TLR	Toll-like receptor
PAMP	Pathogen-associated molecular pattern
DAMP	Damage-associated molecular pattern
LPS	Lipopolysaccharide
IFN-γ	Interferon gamma

IL-4	Interleukin-4
IL-13	Interleukin-13
TGF β	Transforming growth factor β
iNOS	Inducible nitric oxide synthase
JAK	Janus protein kinase
STAT6	Signal and activator of transcription 6
BMDM	Bone marrow-derived macrophage

List of Figures

List of tables

1.0 INTRODUCTION

1.1 History of Choline

Choline, a tertiary amine and essential nutrient (Figure 1), was first identified in the literature by Adolph Strecker in 1862. When conducting experiments boiling animal bile, Strecker discovered a novel nitrogenous compound which he termed “chole” after the Greek word for animal bile (Zeisel, 2012). Despite its early discovery, the metabolic significance of choline remained relatively unknown until Banting and Best isolated insulin from pancreatectomized dogs. During these experiments, Best noticed that the dogs developed significant fat deposition in the liver. Following up on these observations years later, Best conducted new experiments on pancreatectomized dogs and found that the development of fatty liver was corrected by administration of lecithin, now referred to as phosphatidylcholine (PC) (Hershey and Soskin, 1931). Further experiments in rat models showed that fatty liver development was rescued when just choline was administered (Best and Huntsman, 1932, 1935). This early work, which highlighted the role of choline in the regulation of hepatic lipids, reinvigorated the study of choline as an important metabolic molecule.

Although studies in the intervening years showed choline was important to hepatic function in a number of animal models, choline was only classified as an essential nutrient following its study on the impact of human health. Placing patients on a choline-free diet resulted in a decrease in plasma PC and early signs of liver dysfunction, suggesting choline metabolism is important in normal hepatic functioning in humans (Zeisel et al., 1991). This finding was supported by studies performed in patients receiving intravenous feeding which revealed that choline deficiency was related to the development of hepatic steatosis and that

choline supplementation was able to reverse the symptoms (Buchman et al., 1995). These studies led to the Food and Nutrition Board classifying choline as an essential nutrient in 1998 (Zeisel, 2012).

Figure 1. Chemical structure of choline and phosphatidylcholine

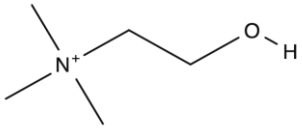

Choline

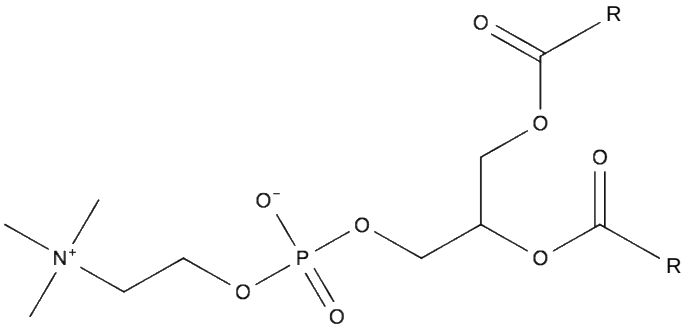

Phosphatidylcholine

1.2 Metabolic Pathways of Choline

In mammals, choline participates in several metabolic pathways that are critical to normal cellular and tissue function. In cholinergic neurons, choline and acetyl-CoA are combined to form the neurotransmitter acetylcholine (Supplemental Figure 1). First, choline is transported into the cell via the high affinity choline transporter (CHT1/SLC5A7) (Haga, 2014; Okuda et al., 2000). In the cytosol, the production of acetylcholine is then catalyzed by choline acetyltransferase (Oda, 1999). Choline and acetylcholine levels are critical factors in normal neurological development, and deficits of either have been shown to cause severe neurological impairment (Ferguson et al., 2004; Fisher et al., 2001).

In the liver and kidney, choline also serves as a substrate for the production of betaine, which occurs in the mitochondria (Supplemental Figure 2). Choline is transported across the mitochondrial membrane where it undergoes two subsequent oxidation steps to form betaine (Jellinek et al., 1959; Ueland, 2011). Once it is transported back into the cytosol, betaine acts as a methyl donor in the betaine-homocysteine S-methyltransferase reaction, which converts homocysteine to methionine (Finkelstein et al., 1983; Obeid, 2013). This pathway has downstream effects on DNA methylation and acts to regenerate tetrahydrofolate for the folate pathway. Abnormal regulation of the folate pathway can cause several diseases including anemia, neural tube defects, and cancer (Christensen et al., 1999; Pogribny et al., 1995). Although choline's role as a substrate for acetylcholine and betaine serve important physiological roles, both represent tissue specific pathways, occurring in cholinergic neurons and the liver and kidney respectively. In eukaryotic cells, choline is predominantly used for the synthesis of PC, the major eukaryotic phospholipid species. PC is synthesized by the cytidine diphosphate choline (CDP)-choline pathway (Figure 2), alternatively known as the

Kennedy pathway after Eugene Kennedy, who elucidated the pathway in 1956. Prior to Kennedy's discovery, the scientific community believed PC was synthesized by direct addition of phosphocholine to phosphatidic acid, a process that was thought to require ATP as a phosphate donor. Upon combining radiolabeled phosphocholine with ATP, phosphatidic acid and rat liver homogenate, no incorporation of the radiolabel into PC was observed (Kennedy and Weiss, 1956). Further experimentation revealed that CDP was necessary for the phosphocholine incorporation to occur, leading to the discovery of the novel intermediate (CDP) (Kennedy and Weiss, 1956).

Since Kennedy's 1956 experiments, the CDP-choline pathway has been well studied. Intracellular choline is phosphorylated by choline kinase and then converted to cytidine diphosphate choline (CDP)-choline by the enzyme phosphocholine cytidylyltransferase (CCT). Under normal cellular conditions, CCT is the rate limiting step in the pathway (Post et al., 1982). CDP-choline is then combined with diacylglycerol (DAG) to create PC, which is catalyzed by choline phosphotransferase (CPT). While the phosphorylation of choline takes place in the cytosol, the final two steps occur affixed to the endoplasmic reticulum and the Golgi body respectively (Henneberry et al., 2002; Lykidis et al., 1999). Although the majority of cellular choline is integrated into PC, choline also exists as the head group to sphingomyelin, which contributes to cellular migration, transduction, and autophagy (Taniguchi and Okazaki, 2014; Young et al., 2013).

Figure 2. Metabolic pathways of *de novo* phosphatidylcholine synthesis.

CK – choline kinase; DAG – diacylglycerol; CCT - phosphocholine cytidylyltransferase; CPT – choline phosphotransferase; PC – phosphatidylcholine; PE – phosphatidylethanolamine; PEMT - phosphatidylethanolamine N-methyltransferase; SAM – S-adenosylmethionine; SAH – S-adenosylhomocysteine.

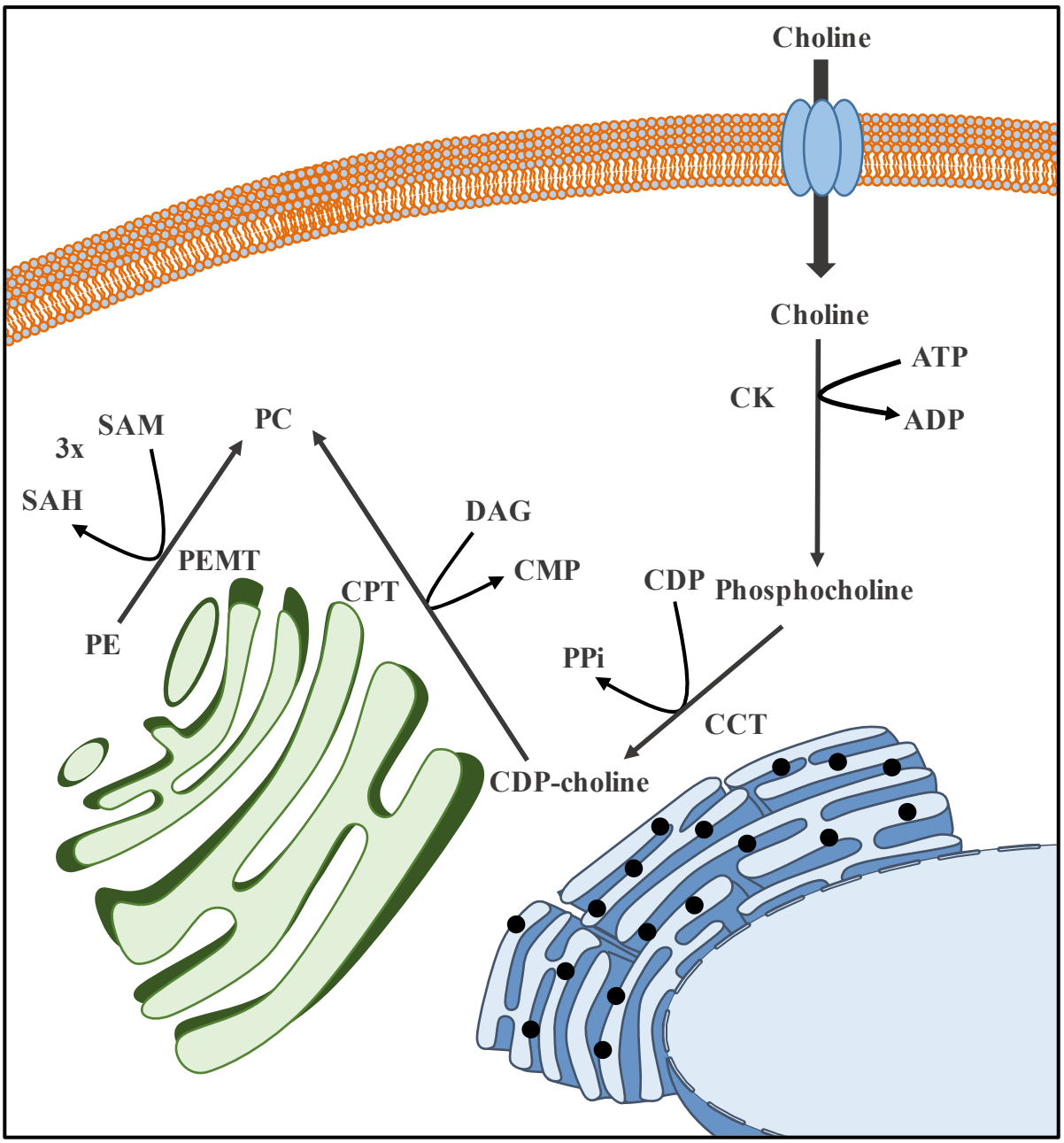
Choline
Choline
ATP
CK
ADP
SAM
3x
PC
SAH
DAG
PEMT
CMP
CPT
CDP
Phosphocholine
PE
PPi
CCT
CDP-choline

Although the Kennedy pathway is the main source of *de novo* PC synthesis, hepatocytes can also generate PC from phosphatidylethanolamine (PE). This process, which is catalyzed by phosphatidylethanolamine N-methyltransferase (PEMT) involves the addition of three sequential methyl groups on the ethanolamine head group of PE to effectively convert the PE molecule to PC (Vance et al., 1997). Although the PEMT contributes to as much as 30% of PC in the liver and adipose tissue, its activity is believed to be limited elsewhere (Cole and Vance, 2010; Vance et al., 1997). Phospholipid restructuring through the Land's pathway provides another method of PC synthesis from existing phospholipid species. In this reaction, phospholipase A catalyzes the removal of an acyl chain from PC, creating lysophosphatidylcholine (lysoPC) and a fatty acid moiety (Linkous and Yazlovitskaya, 2010). Re-acylation is catalyzed by lysoPC acetyltransferases (Frohlich et al., 1982). Base-exchange reactions, which interconvert head groups between phospholipid species can also generate novel PC. However, since PC is the major phospholipid species found in cells, base exchange reactions are generally used to create other phospholipid species from PC, such as phosphatidylserine and PE (Gaiti et al., 1976).

1.3 PC in biological membranes and lipid homeostasis

As the predominant phospholipid found in cells, PC plays a vital role maintaining the structural integrity of biological membranes and in vesicular trafficking and storage critical to metabolic functioning. In eukaryotic cells, PC and PE are the predominant phospholipid species in the outer and inner membranes respectively. The PC to PE ratio in biological membranes is a key determinant in membrane fluidity and permeability (Dawaliby et al., 2016; Li et al., 2006). PC also influences the proliferative capacity of cells, with the up-regulation of choline transporters and Kennedy pathway enzymes important elements in cancer

development (Glunde et al., 2011; Inazu, 2014; Iorio et al., 2010). The significance of choline metabolism in cell growth has led to the use of fluorescent-conjugated and radiolabeled ^{11}C choline in the imaging and diagnosis of various cancers (Buroni et al., 2015; Chotipanich et al., 2016; Giovannini et al., 2015; Reske et al., 2006).

Metabolically, PC is an important intermediate that helps deal with increased lipid burden promoted by a high fat diet. Due to the fatty acyl groups attached to it, PC can act as a fatty acid reservoir (Jackowski et al., 2000). Lipidomic analysis has shown that the acyl groups in DAG are similar to PC, but not PE under metabolic stress (Chitraju et al., 2012). PC is also an important regulator in the storage of neutral lipids. In response to a high fat diet, PC synthesis increases to accommodate an increased lipid burden on cells (Krahmer et al., 2011; Moessinger et al., 2014). Reduction of biosynthetic flux through the Kennedy pathway leads to an increase in lipid droplet size and redirects fatty acids towards incorporation into other neutral lipid species (Jackowski et al., 2000; Krahmer et al., 2011; Moessinger et al., 2014). PC is also a primary component of lipoprotein molecules. PC depletion has been shown to be atheroprotective due to the decreased release of very low density lipoprotein by the liver (Cole et al., 2012; Zhao et al., 2009). PC's comprehensive role in several metabolic pathways highlights its importance in maintaining lipid homeostasis.

1.4 Choline Transport

Due to its positive charge, choline uptake requires transport proteins to facilitate its entry into cells. To date, three classes of transport proteins have been identified. In cholinergic neurons, high-affinity choline transport occurs via the choline specific transporter CHT1 (Haga, 2014; Okuda et al., 2000). Choline transport with CHT1 is the rate-limiting step in acetylcholine synthesis and is thought to provide choline primarily for use in the synthesis of

acetylcholine (Marchbanks and Kessler, 1982). Mice lacking CHT1 are unable to effectively transmit neuronal signals and die shortly after birth (Ferguson et al., 2004). CHT1 is dependent on the presence of sodium and glucose, and is strongly inhibited by hemicholinium-3 (HC-3), a choline analog (Haga, 2014). Due to its role in acetylcholine synthesis and its lack of expression in other cell types, it is not believed that CHT1 contributes significantly to choline uptake in somatic cells (Michel et al., 2006). Choline transport is also facilitated by the organic cation transporter (OCT/SLC22A) family. OCTs are generic transporters of heavy metals and organic cations that have the ability to transport many different structurally distinct compounds (Pelis and Wright, 2014; Sweet et al., 2001). Unlike CHT1, OCTs are not dependent on sodium or glucose and are not inhibited by HC-3 (Sweet et al., 2001). OCT1 and OCT2 have shown the ability to transport choline, however this transport occurs at a low rate and specificity (Gorboulev et al., 1997; Sweet et al., 2001). Despite their ability to transport choline, the role OCTs play in choline metabolism is not well understood.

1.5 Choline Transporter-Like Proteins

At the turn of the 21st century, choline had only recently been recognized as an essential nutrient, but its transport into neuronal cells and use in the acetylcholine pathway had been well established. However, the mechanism by which choline was transported into the non-neuronal cells was not well characterized. Although OCTs are expressed in several tissues and have the capacity to transport choline, their lack of specificity for choline made their involvement in choline's metabolic functions unlikely (Friedrich et al., 2001). In 2000, O'Regan *et al.* discovered a novel transporter while performing complementation studies in yeast (O'Regan et al., 2000). This transporter, which rescued choline uptake from mutant yeast, was sodium independent and sensitive to HC-3 inhibition, traits that excluded the possibility

of OCT or CHT1 transport (O'Regan et al., 2000). Due to its functional overlap with CHT1, the new choline transporter was named the choline transporter-like protein (CTLs).

Shortly after the discovery of the CTL family, it was determined through sequence analysis that the CDw92 protein expressed on the surface of leukocytes was the same protein discovered by O'Regan *et al.* (Wille et al., 2001). Initial reports failed to identify a mouse homologue to CTL1; however this changed in 2004 when Yuan *et al.* discovered a mouse gene encoding CTL1 in muscle. In this study, RNA expression was observed in the brain, skeletal muscle, heart, and testis (Yuan et al., 2004). Further, transfecting Cos-7 cells with CTL1 increased choline uptake, providing additional support for CTL1 as a choline transporter (Yuan et al., 2004). Study of the human CTL1 gene revealed that two splice variants existed for CTL1, designated CTL1a and CTL1b, and that both variants were expressed in the brain, kidneys, heart, placenta, and liver (Yuan et al., 2006).

Since its initial discovery and characterization, several studies have investigated the expression of CTL1 and functional implications in choline transport. The CTL family consists of five isoforms (CTL1-5), with CTL1 and CTL2 primarily responsible for mediating choline uptake (Traiffort et al., 2013). CTL1 is ubiquitously expressed and has been validated as a membrane transporter in the lung, liver, muscle, brain, spinal cord, and hematopoietic compartment (Fujita et al., 2006; Fullerton et al., 2006; Inazu et al., 2005; Ishiguro et al., 2008; Michel and Bakovic, 2009). CTL1 has also been found on the mitochondrial membrane; however its specific role in betaine synthesis has yet to be determined (Michel and Bakovic, 2009). Strong evidence exists suggesting choline uptake via CTL1 is important for cell growth and proliferation. Following motor-neuron injury, CTL1 mRNA and protein is up-regulated *in situ*, suggesting choline uptake and integration into PC is necessary for repair (Che et al., 2002). Choline and CTL1's importance for cell growth is also seen in malignant cells. CTL1

inhibition has been shown to decrease cell growth and increases caspase activation in cancerous cell lines (Machova et al., 2009; Nishiyama et al., 2016). Given that CTL1 appears to be ubiquitously expressed and is seemingly important for cell proliferation and growth, it may be the transporter responsible for normal choline metabolism.

While CTL1 is expressed across several tissues and contributes to choline uptake across all tissue types, CTL2 appears to hold a more specialized phenotype related to the inner ear. CTL2 has been shown to be critical in antibody-induced hearing loss, with circulating antibodies in patients recognizing CTL2 in the inner ear (Kommareddi et al., 2009; Nair et al., 2004). Mice harbouring a CTL2 targeted deletion during embryonic development showed progressive hearing loss by 6 months of age (Kommareddi et al., 2015). This hearing loss was caused by hair cell and spiral ganglion cell death in the inner ear, potentially linking the hearing loss phenotype with PC induced cell death (Kommareddi et al., 2015). CTL2 is also expressed in other cell types, however its specific role in cellular function and disease pathology is poorly understood (Beckmann et al., 2015; Flesch et al., 2013).

One of the early characterizations of CTL1 was performed by Wille *et al.* in 2001. In this study, the authors cloned and characterized a protein broadly expressed on the surface of dendritic cells, CDw92. The protein sequence of CDw92 was matched to the published sequence of human CTL1 (Wille et al., 2001). Although its ability to transport choline was not confirmed in this study, it did raise questions about the role of CTL1 in the inflammatory response. Also in the study, Wille *et al.* used the CDw92 antibody VIM15b to measure how antibody occlusion affected cytokine secretion in response to lipopolysaccharide (LPS), a bacterial endotoxin and pro-inflammatory stimulant (Wille et al., 2001). The experiment revealed that VIM15b treatment increased interleukin-10 (IL-10) secretion but did not alter tumour necrosis factor alpha (TNF-α), interleukin 1 beta (IL-1β), or interleukin 12 (IL-12)

production (Wille et al., 2001). Although this study lacked the comprehensive nature to provide valuable conclusions regarding choline metabolism and the immune response, it raised the possibility that choline uptake could influence how immune cells respond to inflammatory stimuli.

1.6 Macrophage Polarization

Macrophages are phagocytic cells that digest foreign materials and pathogens that play a critical role in the innate immune response. Host macrophages express pattern recognition receptors that recognize either pathogen-associated molecular patterns (PAMPs) or damage-associated molecular patterns (DAMPS) in response to infection or cellular damage respectfully (Kawasaki and Kawai, 2014). Different inflammatory signals are propagated through host cells depending on the type of PRR activated and the type of inflammatory molecule that binds it (Bianchi, 2007).

Classically, macrophages are activated by inflammatory stimuli that promote either a pro-inflammatory (M1, also known as classical activation) state or an anti-inflammatory (M2, also known as alternative activation) state (Figure 3). Classical activation can be stimulated by pro-inflammatory cytokines such as TNF and interferon gamma (IFNγ) as well as bacterial endotoxins such as LPS (Gordon and Taylor, 2005). Binding of these pro-inflammatory factors result in the synthesis and release of pro-inflammatory cytokines such as TNF, interleukin-6 (IL-6), and IL-1β, which further propagates pro-inflammatory signaling (Gordon and Taylor, 2005). Alternatively, M2 macrophages can be subdivided into different groups based on their stimuli and functional responses. M2a macrophages, stimulated by interleukin-4 (IL-4) or interleukin-13 (IL-13), are involved in humoral immunity and parasitic or allergic responses (Gordon, 2003). M2b macrophages, which are stimulated by Fc receptor binding or toll-like

receptor (TLR) signaling, are directly involved in immune regulation (Arango Duque and Descoteaux, 2014). The third class of M2 macrophages are M2c activated cells, which regulate tissue repair and immune suppression are stimulated by IL-10, transforming growth factor beta (TGF-β), or glucocorticoids (Arango Duque and Descoteaux, 2014). Although macrophages are still often referred to under classical terms, it is now widely recognized that macrophage polarization exists as a continuous spectrum able to respond to different factors simultaneously rather than occupying an individual polarization state (Italiani and Boraschi, 2014).

Metabolic reprogramming upon inflammatory stimulation can also play a major role in macrophages' immunological functions. Classically activated macrophages favour aerobic glycolysis to generate ATP, which promotes the production of reactive oxygen species and nitrous oxides to elicit bactericidal responses (Peyssonnaux et al., 2005; Rodriguez-Prados et al., 2010). On the other hand, M2 macrophages favour oxidative metabolism, beta oxidation, and arginase activity, which increase levels of metabolic intermediates important for wound healing (Odegaard and Chawla, 2011; Vats et al., 2006). Due to these metabolic changes, a common metric for determining the polarization state of macrophages is comparing the expression or activity levels of inducible nitric oxide synthase (iNOS) to arginase.

Figure 3. Classical and alternative activation of macrophages.

Naïve monocytes are recruited from circulation into tissues in response to inflammatory signals. Macrophages can be classically activated towards a pro-inflammatory M1 phenotype or alternatively activated towards an M2 phenotype. Although macrophages are traditionally described as either M1 or M2, they exist as part of a continuous spectrum between M1 and M2 like phenotypes. The inflammatory status of macrophages has an impact on metabolism with the ability to influence insulin sensitivity, macrophage localization, and energy storage.

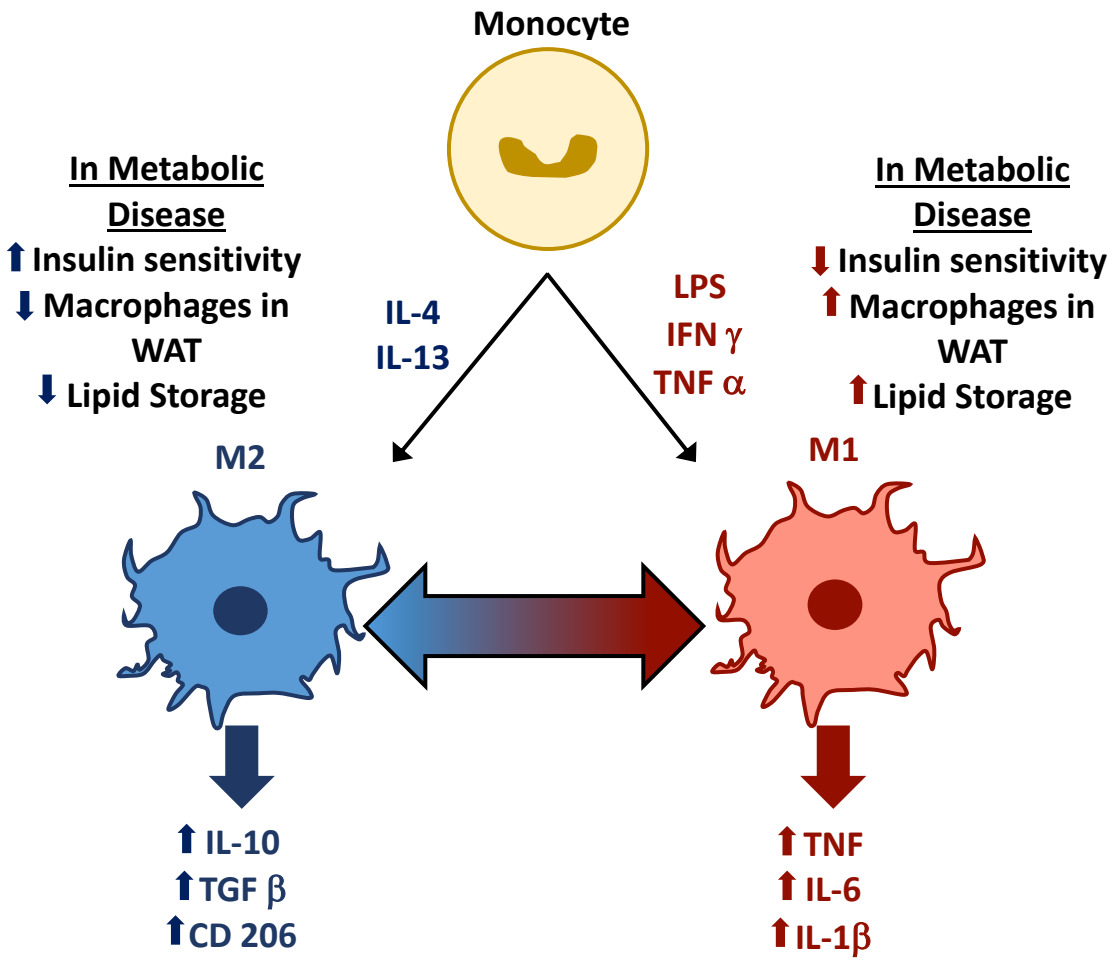
Monocyte
In Metabolic Disease
⬆ Insulin sensitivity
⬇ Macrophages in WAT
⬇ Lipid Storage
IL-4
IL-13
LPS
IFN γ
TNF α
In Metabolic Disease
⬇ Insulin sensitivity
⬆ Macrophages in WAT
⬆ Lipid Storage
M2
M1
⬆ IL-10
⬆ TGF β
⬆ CD 206
⬆ TNF
⬆ IL-6
⬆ IL-1β

1.7 TLR4 Signaling Pathway

One of the most diverse and widely studied families of PRRs are the toll-like receptor (TLR) family. Humans express 10 types of TLRs that elicit a wide variety of intra-cellular and extracellular immune responses (Kawasaki and Kawai, 2014). One of the most intensely studied TLR family members is TLR4, an extracellular receptor to which LPS binds (Chow et al., 1999; Poltorak et al., 1998). Upon TLR4 activation (Supplementary Figure 3), signal transduction can proceed through either the MyD88 dependent or the TRIF pathway (Kawasaki and Kawai, 2014). In the MyD88 pathway or the TRIF dependent pathway, LPS binding initiates the formation of a myddosome consisting of MyD88 and the IRAK family members IRAK4 and IRAK1 (Lin et al., 2010). The autophosphorylation of IRAK1 allows for its release and association with TRAF6 ubiquitin ligase (Ye et al., 2002). This promotes the activation of TAK1 which subsequently activates both the IKK-NFκB pathway and the MAPK pathway (Karin and Gallagher, 2009; Takaesu et al., 2003; Yamazaki et al., 2009). IKK phosphorylation of IKβα promotes NFκB translocation to the nucleus where it binds DNA to promote the synthesis of pro-inflammatory genes (Mercurio et al., 1997). Alternatively, signal transduction through TRIF activates two separate pathways via RIP-1 and TRAF3 (Yamamoto et al., 2003). RIP-1 activates the NFκB pathway via TAK1 activation, while TRAF3 activation leads to IRF3 phosphorylation and translocation to the nucleus, resulting in the transcription of type I interferon (Fitzgerald et al., 2003; Yamamoto et al., 2003). Activation of the TRIF and MyD88 pathways through TLR4 represent one of the major mechanisms of pro-inflammatory signaling.

1.8 IL-4 Signaling Pathway

Much like pro-inflammatory signaling pathways, alternative activation can occur through several different signal transduction cascades. One of the main mechanisms of M2 polarization occurs via IL-4 binding to its receptor, the IL-4 receptor (IL-4R) (Supplementary Figure 4). IL-4R is a heterodimer composed of an α domain, which binds IL-4, and a γ_c chain (Kondo et al., 1993). Upon IL-4 binding to IL-4R, receptor dimerization occurs and promotes the activation of Janus protein kinases (JAK1 and JAK3) (Malabarba et al., 1995; Nelms et al., 1999; Oakes et al., 1996). JAK proteins phosphorylate the cytoplasmic end of the IL-4 receptor, which leads to the activation and translocation of signal and activator of transcription 6 (STAT6) (Chatila, 2004; Hou et al., 1994; Ryan et al., 1998). STAT6 activity is responsible for the majority of IL-4's inflammatory responses, with its knockout eliminating IL-4 dependent functions such as IgE production and lymphocyte differentiation into Th2 cells (Kaplan et al., 1996). IL-4 binding also promotes the recruitment and activation of insulin receptor substrate, which leads to a signaling cascade that activates phosphoinositide 3-kinase and Akt (Nelms et al., 1999; Wang et al., 1993) . This pathway is thought to be responsible for mediating proliferative signals in immune cells (Wurster et al., 2002).

1.9 Role of Classical Activation in Metabolic Disease

Although inflammation is principally responsible for protecting cells against pathogens and responding to cellular damage, it also significantly impacts metabolic regulation. Under normal metabolic conditions, adipose tissue consists of a small population of tissue associated macrophages that skew towards an M2-like state (Castoldi et al., 2015). With the development of obesity, these macrophages become M1 polarized and help exacerbate inflammation through macrophage recruitment and cytokine secretion (Castoldi et al., 2015; Chawla et al.,

2011; McNelis and Olefsky, 2014). These immunological changes have negative whole-body physiological effects, affecting insulin resistance and lipid accumulation in peripheral tissues (Chawla et al., 2011; McNelis and Olefsky, 2014).

One of the first papers to suggest a link between inflammatory signaling pathways and metabolic disease examined the role TNF-α in various strains of obese mouse models (Hotamisligil et al., 1993). Relative to their lean mice counterparts, obese mice showed elevated levels of TNF-α (Hotamisligil et al., 1993). In addition, TNF-α treatment on cultured adipocytes revealed a similar reduction of Glut4 expression seen in obese mice, indicating a change in glucose responsiveness was occurring in response to TNF-α treatment (Hotamisligil et al., 1993). Finally, they showed that treatment with TNF receptor IgG increased peripheral glucose uptake, indicating increased insulin sensitivity (Hotamisligil et al., 1993). The publication of this study established inflammation in adipocytes as a critical component of metabolic dysfunction.

The link between inflammation and metabolism was further strengthened by Weisberg *et al.*'s 2003 paper in the Journal of Clinical Investigation, which implicated adipose tissue macrophages as a critical mediator of increased pro-inflammatory signaling in obesity. In their study, they observed an increase in F4/80 expression during obesity, which corresponded to an increase in macrophage infiltration from 10% in lean state mice to 40% in obese mice (Weisberg et al., 2003). They also determined that the $F4/80^{+}$ cells localized to the adipose tissue were responsible for producing pro-inflammatory factors such as TNF-α, IL-6, and inducible nitrogen oxide synthase (iNOS) (Weisberg et al., 2003). These findings suggested there was an association between classical activation of macrophages and the development of obesity.

Several findings have since supported the link between classical macrophage activation and obesity. Mice fed a high fat diet exhibit chronic low-grade inflammation induced by LPS (Cani et al., 2007). Upon deletion of the LPS co-receptor CD14, mice show reduced plasma insulin concentrations and a lower weight of adipose and liver tissue (Cani et al., 2007). In addition, metabolites indicative of hyperlipidemia induce a strong pro-inflammatory response. Oxidized low-density lipoprotein and saturated fatty acids, both of which are elevated in hyperlipidemia, are activators of TLR4 (Howell et al., 2011; Kiyan et al., 2014). Knockout of TLR4 from hematopoietic cells show increased insulin responsiveness when challenged with saturated fatty acids (Shi et al., 2006). It has also been separately shown that TLR4 knockout promotes alternative activation of macrophages and reduced adipose tissue inflammation (Orr et al., 2012). These studies reveal that pro-inflammatory signaling, which can be initiated by traditional PAMPs or metabolic constituents like free fatty acids, play a central role in the development of obesity and related metabolic diseases.

1.10 The alternative activation of macrophages improves status of metabolic disease

Since increased pro-inflammatory signaling is associated with poorer outcomes in metabolic disease, many investigators have contemplated whether a change in macrophage polarization status could help ameliorate the diseased state. A 2007 study by Lumeng *et al.* investigated the link between alternative activation of macrophages and diet induced obesity in wild-type mice. While lean mice show significant expression of alternative activation markers, diet induced obesity causes a marked reduction in these factors (Kang et al., 2008; Lumeng et al., 2007). Furthermore, pre-treatment with IL-10 restores insulin signaling and sensitivity in TNF-α induced adipocytes (Lumeng et al., 2007). Similar findings have validated the relationship between alternative activation and improvement in obesity and

insulin signaling. When PPARδ signaling, which promotes M2 polarization, is knocked out, mice exhibit increased pro-inflammatory signaling, insulin resistance, and macrophage localization in white adipose tissue, all of which are indicators of metabolic disease (Kang et al., 2008). Due to its role in STAT6 signaling, studies have suggested that IL-4 could play a crucial role improving metabolic disease. Chronic IL-4 treatment reduced weight gain and improved glucose tolerance in mice (Chang et al., 2012). IL-4 also causes increased lipolysis in mice, which potentially explains the decreased weight gain (Tsao et al., 2014). With the vast number of studies showing the importance of inflammation in the progression of obesity and insulin resistance, developing mechanisms of modulating inflammation presents a viable therapeutic in treating metabolic disease.

1.11 Relationship between choline metabolism and inflammation

Due to the impact inflammatory signaling has on metabolic functioning, it is important to understand the interplay between metabolism and inflammation. As the first and potentially rate-limiting step in PC metabolism, choline uptake could potentially regulate macrophage immune responses. Despite the potential link, few papers have examined the relationship between choline uptake, PC synthesis and inflammation. Studies have demonstrated that LPS stimulation increases the incorporation of radiolabeled choline into PC (Chu, 1992; Grove et al., 1990). This increase may suggest that increasing PC content is important for mediating an inflammatory response. The impact of inflammatory stimuli on choline uptake and the influence of the alternative activation of macrophages on choline uptake and metabolism are unknown.

In 2006, Fullerton *et al.* investigated choline uptake during the transition of THP-1 monocytes to macrophages. Over the course of differentiation into macrophages, THP-1

monocytes show reduced choline uptake and have a decreased maximal rate of choline uptake (Fullerton et al., 2006). This change is caused by an internalization of the choline transporter CTL1 from the cell membrane (Fullerton et al., 2006). This finding suggests that monocytes reduce choline uptake following differentiation, which may have the effect of decreasing PC synthesis, which would contradict the previous findings regarding LPS stimulation and choline incorporation into PC.

The most significant link between choline metabolism and inflammation was made when cytokine secretion from CCT-α (the rate-limiting step in PC synthesis) null macrophages were examined. The CCT-α mouse model, which showed a marked reduction in PC and total CCT activity, had a reduced capacity to secrete inflammatory cytokines TNF-α and IL-6 into culture media in response to LPS (Tian et al., 2008). Cytosolic accumulation of both TNF-α and IL-6 was observed following LPS treatments, which prevented CCT-α null mice from mounting a sufficient bacterial response (Tian et al., 2008). Exogenous lysoPC restored normal inflammatory secretion, which lead the researchers to conclude PC is necessary for cytokine secretion (Tian et al., 2008). Although CCT knockout decreased cytokine output, no study has examined the direct effects of choline uptake on cytokine secretion.

2.0 RATIONALE

Macrophage polarization and inflammatory signaling has been shown to influence metabolic outcomes such as insulin sensitivity, macrophage localization, and lipid storage. Due to its role as a critical lipid intermediate and an important component of biological membranes, studies have investigated the influence of choline metabolism and PC in inflammation. Although PC has been shown as an important mediator of the inflammatory response, the relationship between choline uptake and inflammation has yet to be sufficiently addressed.

3.0 HYPOTHESIS

I hypothesize that macrophage polarization will increase choline uptake and PC synthesis and that inhibiting choline transport will inhibit cytokine release in response to immune stimuli, and that both of these events will occur in a CTL1 dependent fashion.

4.0 OBJECTIVES

4.1 Objective 1 – Characterize the effect of macrophage polarization on choline metabolism

Limited studies have investigated the relationship between inflammation and choline metabolism. The purpose of my first objective was to determine the effect of macrophage polarization on choline uptake and incorporation into lipids in primary murine bone marrow-derived macrophages (BMDM). After addressing the influence of macrophage polarization on choline uptake, I investigated whether altering the polarization status affected choline transporter expression.

4.2 Objective 2 – Characterize the effect of choline deficiency on macrophage inflammation

Deficiency in the CDP-choline pathway via deletion of CCTα, which catalyzes the rate-limiting step in PC synthesis, has been shown to inhibit cytokine secretion. The goal of my second objective is to determine whether inhibiting choline uptake influences an LPS-mediated inflammatory response. To model choline deficiency, choline uptake in BMDM was chronically reduced with choline uptake inhibitors and CTL1 antibodies. Once choline deficiency was induced, cells were exposed to an acute dose of LPS and cytokine secretion of IL-6, TNF-α, and IL-10 were assessed. The goal of this objective was to determine if choline deficiency could modulate the inflammatory response in BMDM.

5.0 METHODS

5.1 Murine bone marrow-derived macrophage isolation and culture

Bone marrow-derived macrophages were obtained by culturing bone marrow cells from C57BL/6 mice. These cells were differentiated into macrophages using L929 conditioned media, which contains the growth factor macrophage colony-stimulating factor. L929 media was made by culturing L929 cells for 10 days in Dulbecco's modified eagle medium (DMEM with 4.5 g/L of glucose, with L-glutamine and sodium pyruvate, Wisent) supplemented with 10% fetal bovine serum (FBS, heat-inactivated, Wisent) and 1% penicillin/streptomycin (Fisher). The conditioned media was prepared by spinning the cells at 3000 rpm and filtering the media through a 0.22 μm filter.

To obtain cells, mice were cervically dislocated and legs were dissected away from the body at the hip joint. Bones were cleaned of all muscle and separated into the femur and tibia, which were each cut at both ends to expose the bone marrow. Bones were then placed inside a 0.5 mL tube with a hole punctured in the bottom by an 18-gauge needle. Next, the 0.5 mL tube was placed inside a larger 1.7 mL tube with 100 μL of media. Bone marrow cells were obtained by centrifugation of the 1.7 mL tube at 5000 rpm. Cells were re-suspended in 1 mL of media and filtered through a 0.45 μm filter to remove any debris. Following an overnight culture (37°C and 5% CO_2) in 85 mL of culture media (DMEM with 10% FBS and 1% Penicillin/streptomycin) 15 mL of L929 conditioned media was added. Cells were plated in 10 cm dishes and allowed to differentiate. Cell adhesion to plates indicated differentiation and occurred at day 6-7.

5.2 LPS/IL-4 treatment and rate of choline uptake

For all choline uptake and incorporation experiments, BMDM were plated in 24-well cell culture dishes (250,000 cells/well). BMDM were treated for 48 hours with LPS (from *E. coli:B4*, Sigma-Aldrich, 100 ng/ml) or IL-4 (mouse recombinant IL-4, R&D, 20 ng/ml) in normal culture media. A 48-hour time interval was chosen to allow for polarization of macrophages into either a pro or anti-inflammatory state. The rate of choline uptake was determined by measuring ^{3}H-choline chloride (Perkin Elmer) taken up into cells. One hour prior to uptake, cells were incubated in Krebs-Ringer-HEPES buffer (KRH, 130 mM NaCl, 1.3 mM KCl, 2.2 mM $CaCl_2$, 1.2 mM $MgSO_4$, 1.2 mM KH_2PO_4, 10 mM HEPES, pH 7.4, and 10 mM glucose) to remove exogenous choline. Immediately prior to uptake, cells were washed again with 300 μL of KRH buffer. Then, KRH buffer containing 1 μCi/mL of ^{3}H-choline chloride was added and cells were incubated at 37°C for desired time point (1-30 minutes). Following incubation, cells were washed twice with KRH buffer, lysed in 150 μL of 0.1 M NaOH and freeze-thawed at -80°C. A 50 μL aliquot was added to 5 mL of scintillation fluid (Ultima Gold™ Scintillation Cocktail, Perkin Elmer) and radioactivity was measured on a beta-scintillation counter (Tri-Carb 2910TR, Perkin Elmer). Based on the concentration of the radioactive solution (83 Ci/mmol), DPM counts were converted to μmol choline and expressed as a function of time.

5.3 Choline uptake kinetics

Choline uptake kinetic parameters were determined by creating a Michaelis-Menten curve. BMDM were polarized for 48 hours with LPS (100 ng/ml) or IL-4 (20 ng/ml) in normal culture media. Since the rate of choline uptake in BMDM is linear over the first 10 minutes, a 10 minute uptake interval was selected as the approximation of the initial rate. Cells were incubated in KRH buffer for one hour prior to uptake and washed twice with buffer immediately before. Cells were then incubated for 10 minutes in KRH buffer with 1 μCi/mL of ^{3}H-choline chloride and various concentrations of unlabeled choline chloride (5-200 μM). Following incubation, cells were washed twice with KRH buffer, lysed in 150 μL of 0.1 M NaOH and freeze-thawed at -80°C. A 50μL aliquot was added to 5 mL of scintillation fluid and radioactivity was measured on a beta-scintillation counter. The DPM counts from the scintillation counter were converted to μmol choline and expressed as a function of time.

5.4 Choline uptake HC-3 sensitivity

Hemicholinium-3 (HC-3) IC_{50} curves were generated to measure the amount of choline-specific uptake occurring in macrophages. BMDM were polarized for 48 hours with LPS (100 ng/ml) or IL-4 (20 ng/ml) in normal culture media. Cells were incubated in KRH buffer for one hour prior to uptake and washed twice with buffer immediately before. Cells were then incubated for 10 minutes in KRH buffer with 1 μCi/mL of ^{3}H-choline chloride and various concentrations of HC-3 (0.1 μM to 10 mM, Sigma-Aldrich). Following incubation, cells were washed twice with KRH buffer, lysed in 150 μL of 0.1 M NaOH and freeze-thawed at -80°C. Protein in cell lysate was determined using the BCA protein assay. An aliquot of cell lysate was added to 5 mL of scintillation fluid and radioactivity was measured on a beta-

scintillation counter. Uptake values were standardized to protein and expressed as a percentage of untreated control.

5.5 Choline incorporation into lipids

BMDM were incubated with DMEM in the presence of LPS (100 ng/mL), IL-4 (20 ng/mL), or untreated DMEM for 48 hours prior to radioactive treatment. Following inflammatory treatment, cells were washed with phosphate-buffered saline (PBS, 137 mM NaCl, 2.7 mM KCl, 8.1 mM Na_2HPO_4, 1.5 mM KH_2PO_4) and treated with media containing 1 μCi/mL ^{3}H-choline chloride for 2,4,6, and 8 hours. Cells were then washed twice with PBS and lysed with a freeze thaw cycle at -80°C in 200 μL of PBS. Lipids were extracted from whole cell lysate using the Bligh and Dyer method (Bligh and Dyer, 1959). After resolution of the phases, the radioactivity in the lower chloroform phase containing the neutral lipid fraction was measured using a beta-scintillation counter. All radioactive measurements were standardized to total protein as measured by a BCA assay.

5.6 HC-3 and DMAE inhibited choline uptake and incorporation

Choline uptake inhibitors HC-3 and 2-dimethylaminoethanol (DMAE), Sigma Aldrich) were used to determine the effect of inhibition of choline-specific uptake mechanisms on the synthesis of PC. BMDM were incubated in KRH buffer one hour prior to uptake. Then, cells were washed twice with buffer to ensure the removal of exogenous choline. Uptake of 1 μCi/mL ^{3}H-choline chloride in KRH buffer was measured over ten minutes at 37°C in the presence of 250 μM HC-3, 500 μM DMAE, or a vehicle control. After the incubation, cells were washed twice with KRH buffer and lysed in Following incubation, cells were washed twice with KRH buffer, lysed in 150 μL of 0.1 M NaOH and freeze-thawed at -80°C. Protein in cell lysate was determined using the BCA protein assay (Thermo Fisher) and absorbance

was read on a Synergy H1 microplate reader (BioTek). An aliquot of cell lysate was added to 5 mL of scintillation fluid and radioactivity was measured on a beta-scintillation counter. The DPM counts from the scintillation counter were converted to μmol choline and standardized to protein amounts from BCA assay.

Choline incorporation into lipids in the presence of choline uptake inhibitors was examined by incubating BMDM in full DMEM media containing 1 μCi/mL of ^{3}H-choline chloride and 250 μM HC-3, 500 μM DMAE, or a DMSO control for 48 hours (37°C, 5% CO_2). After incubation, cells were washed twice with PBS and lysed with a freeze-thaw cycle at -80°C in 200 μL PBS. Whole cell lysate was then extracted using the Bligh and Dyer method. A 50 μL aliquot of the lipid phase was counted for radioactivity using a beta scintillation counter. DPM counts were standardized to protein counts acquired from the inhibitor uptake analysis.

5.7 CTL1 antibody treated uptake and incorporation

The role of CTL1 in choline uptake and incorporation in BMDM was addressed by treating cells with CTL1 antibodies. Antibodies were obtained from the Bakovic group (Department of Human Health and Nutritional Sciences, University of Guelph). Two antibodies were used; LV-58, which is specific for the N terminus of the protein, and EN-627, which is specific for the C terminus of the protein. Prior to uptake, cells were incubated in KRH buffer containing a 1/100 dilution of each antibody stock (concentration unspecified), as well as an untreated and an IgG antibody control. Cells were washed twice immediately prior to uptake. Choline uptake was measured by incubating cells in 1 μCi/mL ^{3}H-choline chloride in KRH buffer for 10 minutes (37°C, 5% CO_2). Cells were washed twice with buffer to remove

radioactivity and lysed in 0.1 M NaOH. Following incubation, cells were washed twice with KRH buffer, lysed in 150 μL of 0.1 M NaOH and freeze-thawed at -80°C.

Choline incorporation into lipids in the presence of antibodies was measured by incubating BMDM with full DMEM containing 1μCi/mL ^{3}H-choline chloride and a 1/100 dilution of each antibody stock for 48 hours. Untreated and IgG treated cells were used as negative controls. After incubation, cells were washed twice with PBS and lysed with a freeze-thaw cycle at -80°C in 200 μL PBS. Whole cell lysate was then extracted using the Bligh and Dyer method. A 50 μL aliquot was counted for radioactivity using a beta scintillation counter. DPM counts were standardized to protein counts acquired from the inhibitor uptake analysis.

5.8 Choline depletion and cytokine secretion

BMDM were choline depleted using either choline uptake inhibitors or through CTL1 antibody occlusion. Normal culture media was supplemented with 250 μM HC-3, 500μM DMAE, a 1/100 dilution of the C-terminal or N-terminal antibody, or a vehicle control and cells were incubated for 48 hours (37°C, 5% CO_2). Following choline depletion, cells were washed with PBS and treated with LPS (100 ng/mL) or normal culture media for 6 hours. Choline uptake inhibitors were present in the same concentrations during LPS treatments, while CTL1 antibodies were not re-incubated during LPS treatment. After LPS treatment, media was transferred to 96-well plates and stored at -80°C.

Duoset ELISA kits (R&D Systems) were used to measure cytokine secretion. Cytokines (TNF-α, IL-6, IL-10, IL-β) were all measured using the same method according to the manufacturer's instructions. 96-well ELISA plates were coated with 100 μl of the respective capture antibody (prepared in PBS, 800 ng/mL for TNF-α, 2 μg/mL for IL-6, and 4μg/mL for IL-10) overnight at room temperature. The next day, cells plates were decanted

and washed 3 times with wash buffer (0.05% Tween® 20 in PBS). Next, plates were blocked with reagent diluent (1% bovine serum albumin (BSA,) in PBS) for 1 hour. Following the incubation, reagent diluent was removed and wells were washed 3 times with wash buffer. The plate was then incubated with experimental samples diluted in reagent diluent (5-fold dilution for TNF-α, 2-fold dilution for IL-6, IL-10, and IL-1β) for 2 hours. Plates were washed 3 times with wash buffer and samples were incubated in 100 μL of detection antibody (prepared in reagent diluent, 800 ng/mL for TNF-α, 2 μg/mL for IL-6, and 4 μg/mL for IL-10) for 2 hours. Following the incubation, detection antibody was decanted and plates were washed 3 times with wash buffer. Cells were incubated in streptavidin-HRP conjugated to horseradish-peroxidase for 20 minutes in the dark and subsequently washed 3 times with wash buffer. Next, plates were visualized by incubating wells in 100 μL of substrate solution (1:1 mixture of hydrogen peroxide and tetramethylbenzidine, R&D Systems) for 20 minutes. Visualization was stopped by adding 50 μL of 2N H_2SO_4. Absorbance readings were obtained at 450 nm using a microplate reader and unknown values were calculated using a standard curve fitted using a four-parameter logistic curve fit using Prism 6 software (GraphPad Software Inc.).

5.9 RNA isolation, cDNA synthesis and qPCR

RNA was isolated from BMDM in 12 well plates according to the TriPure reagent protocol (Roche Life Sciences). Isolated RNA was re-suspended in 30 μL of RNAse/DNAse free water (Wisent). RNA concentration and purity was determined by measuring absorbance of RNA at 260/280 nm using a Take3 plate (BioTek). Samples were equalized to the lowest RNA concentration with RNAse/DNAse free water. First strand of cDNA was synthesized using the QuantiNova™reverse transcription kit (Qiagen) according to kit instructions except in half the reaction volume. Briefly, 6 μL of isolated RNA was incubated with 1μL of gDNA

removal buffer and incubated at 45°C for 2 minutes. Then, 3 μL of master mix containing 1:4 ratio of reverse-transcription master mix:reverse transcriptase was added to each RNA sample. Prepared RNA solutions were incubated on a thermal cycler (BioRad T100 Thermal Cycler) according to kit cycling conditions (25° for 3 min, 45°C for 10 min, then 85°C for 5 min). The newly synthesized cDNA strand was diluted 1:40 in water. Diluted cDNA was used for real-time PCR using the QuantiNova™Probe PCR kit according to manufacturer's instructions except volumes reduced by half. Briefly, 5 μL of kit master mix and 0.25 μL of TaqMan primer (primer list and details included in Supplementary Table 1) were added to 4.75 μL of diluted cDNA. Samples were cycled for 40 cycles according to the manufacturer's instructions using the Roto-Gene Q series (Qiagen) and the fluorescence was measured. The delta-delta critical threshold method was used for relative expression, where sample threshold values are standardized to an internal standard (β-actin was used) before comparing between treatment groups to determined relative expression (Livak and Schmittgen, 2001).

5.10 Western Blot and Protein Quantification

BMDM were polarized with LPS (100 ng/mL) or IL-4 (20 ng/mL) for 48 hours prior to protein collection. Cells were washed twice with PBS and lysed in a denaturing lysis buffer (50 mM Tris-HCl pH 7.5, 150 mM NaCl, 1 mM EDTA, 0.5% Tritton X-100, 0.5% NP-40, 100 μM sodium orthovanadate). Protein was equalized using the BCA protein assay and equally loaded onto an 8% SDS-PAGE gel where it was run for 90 min at 110V. Gel was transferred onto a PVDF membrane (17 minutes at 1.3 A) using the Trans-Blot® Turbo™ Transfer System (Biorad) with Bjerrum Schafer-Nielsen buffer (48 mM Tris, 39 mM glycine, 20% methanol). Membrane was blocked for 1 hour in 5% BSA then incubated at 4°C overnight in CTL1 primary antibody (EN-627 as specified above) or β-actin rabbit (HRP conjugated,

Cell Signaling). A 1/1000 dilution of stock antibodies in 5% BSA were used for primary antibody incubations. The following day, membranes were washed 4 times in TBST (20 mM Tris, 150 mM NaCl, 0.05% Tween® 20) then CTL1 membrane was incubated for 1 hour in HRP conjugated anti-rabbit IgG (Cell Signaling, 1/5000 dilution). Clarity™ Western ECL solution (BioRad) was applied to membranes which were visualized using LAS 4010 ImageQuant Imaging System (General Electric). Densitometry analysis was performed using ImageJ software (version 1.48) and CTL1 expression was standardized to β-actin internal control.

5.11 Generation of CTL1$^{-/-}$ Mouse Model

The CTL1$^{-/-}$ mouse model was generated by inGenious Targeting Laboratories (Ronkonkoma, New York, United States) using a KOMP targeting vector (Project ID: CSD29103) (Skarnes et al., 2011). Briefly, the vector was electroporated into C57BL/6 embryonic stem cells which were microinjected into Balb/c blastocysts. Chimeras were bred with C57BL/6 to generate heterozygotes for the targeted (floxed) allele. Homozygous floxed mice were crossed to mice expressing Cre recombinase in every tissue (B6.C-Tg(CMV-cre)1Cgn/J- stock number 006054). For the current studies, non-breeding mice generated from F2 crosses were used, in which CTL1 (exon 3) had been deleted, but in which Cre was still expressed.

5.12 CTL1$^{-/-}$ DNA isolation and genotyping

DNA isolation for genotyping was performed by placing clipped tails in a 500 μL mixture containing 495 μL of tail lysis buffer and 5 μL of proteinase K (10 mg/mL, Bioshop)

(100 mM Tris-HCl pH 8, 5 mM EDTA, 200 mM NaCl, 0.2% SDS) and incubating solution overnight at 55°C. The following day, samples were centrifuged for 20 minutes at 13,000 rpm. Following the spin, the supernatant was transferred to a new 1.7 mL tube. 500 μL of isopropanol was added to the tube and samples were incubated at -20°C for 20 minutes. Next, samples were centrifuged for 15 minutes at 13,000 rpm and the supernatant was decanted. The remaining pellets were then washed twice with 700 μL of ethanol before another spin at 13,000 rpm for 5 minutes. Pellets were re-suspended in TE buffer (10 mM Tris-HCl pH 8 and 1mM EDTA) and quantified with the microplate reader on a Take3 plate.

Once samples were equalized, DNA was amplified by PCR using primers specific for the floxed, knockout, at wild type alleles (Supplementary Figure 5). Reactions were set up by adding 0.5 μL of DNA template to 7.45 μL of nuclease free water, 1 μL of PCR buffer (Diamed), 0.2 μL of dNTPs (Diamed), 0.25 μL of each primer, and 0.1 μL of DNA Taq polymerase (Diamed). Samples were set up to run on the thermal cycler according to manufacturer's instructions (94°C for 3 minutes, 36 cycles of 25 s at 94°C, 25 s at 60°C, and 1 minute at 72°C, followed by 72°C for 5 minutes). DNA was then separated on an agarose gel (100 mL of TAE buffer, 1.5 g of agarose, and 5 μL of RedSafe (FroggaBio)) and visualized using the ChemiDoc MP System (BioRad).

5.13 Statistical Analyses

All statistical analyses were performed using Prism 6 (GraphPad Software Inc.). Choline uptake and incorporation data was analyzed using a two-way ANOVA comparing the

treatment group (LPS or IL-4) to the untreated control. Inflammatory cytokine gene expression was analyzed using an unpaired student's t-test. Kinetic curves and values were generated using the Prism 6 non-linear regression Michaelis-Menten curve fit. HC-3 IC_{50} curve and values were fit using Prism 6 non-linear regression vs. response with variable slopes curve fit. CTL1 expression data and choline depleted cytokine uptake, incorporation, and cytokine secretion experiments were analyzed using a one-way ANOVA comparing the treatment groups to the control groups. Statistical analyses were not performed on $CTL1^{-/-}$ experiments due to a lack of sufficient biological replicates. Across all forms of analyses, statistical significance is noted as follows: * $p< 0.05$, ** $p< 0.01$, *** $p< 0.001$, **** $p< 0.0001$.

6.0 RESULTS

6.1 Macrophage polarization increases choline uptake and incorporation

LPS has been previously shown to increase choline incorporation into PC; however, the role of macrophage polarization on choline uptake and metabolism is unknown. Macrophages were polarized for 48 hours with LPS or IL-4 prior to measuring choline uptake and metabolism. Polarization states of macrophages were verified by examining RNA expression of pro-inflammatory or anti-inflammatory markers (Figure 4). In response to LPS, the pro-inflammatory cytokines IL-6, TNF-α, and IL-1β all increased significantly relative to the untreated control. Conversely, IL-4 increased the expression of the anti-inflammatory cytokines transforming growth factor β and cluster of differentiation 206. The ratio of iNOS to arginase expression, which is indicative of macrophage polarization, was also examined. LPS stimulated macrophages exhibited an increased iNOS/arginase ratio, while IL-4 treatment decreased the ratio relative to untreated cells. The induction of appropriate cytokines and the expected levels of arginase and iNOS expression demonstrate that LPS and IL-4 skewed cells towards an M1-like and M2-like state respectively.

Figure 4. LPS and IL-4 induce macrophage polarization in BMDM.

(A) Wild-type BMDM were treated with LPS (100 ng/mL) or IL-4 (20 ng/mL) for 48 hours prior to measuring choline uptake. RNA expression was measured by generating cDNA strands and performing qPCR using the QuantiNova™ qPCR kit. The expression of, iNOS/Arginase **(B)**, TNF α **(C),** IL-6 **(D)**, and IL-1β **(E)** were measured in response to LPS. iNOS/Arginase **(F)**, TGF-β **(G)**, and CD 206 **(H)** were measured in response to IL-4. Expression was set relative to an untreated control using the delta delta Ct method. Statistical analysis was performed using an unpaired t-test (n= 3, * $p<0.05$, *** $p<0.001$, **** $p<0.0001$,)

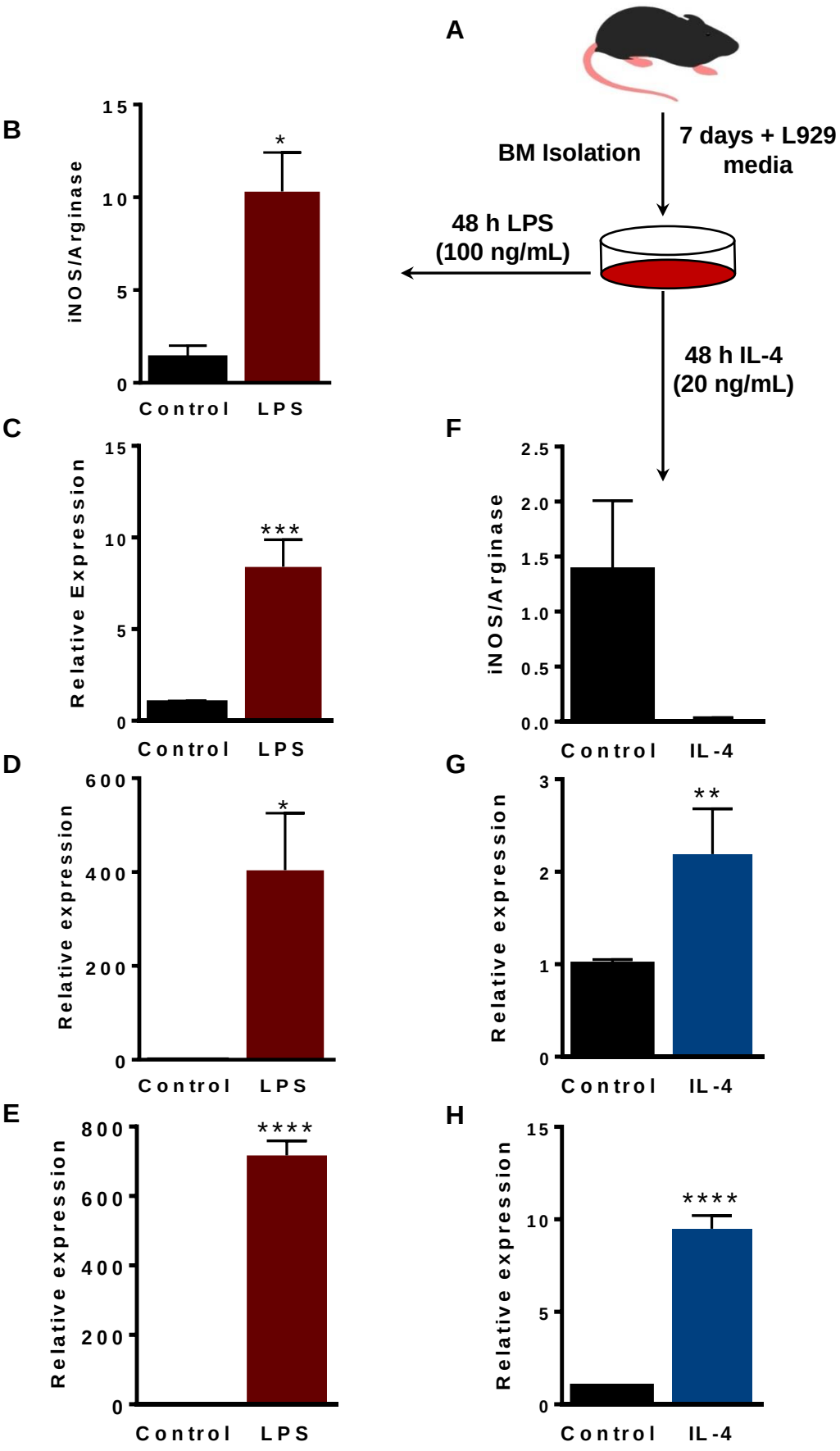
A
BM Isolation
7 days + L929 media
48 h LPS (100 ng/mL)
48 h IL-4 (20 ng/mL)
B
iNOS/Arginase
Control
LPS
C
Relative Expression
D
Relative expression
E
Relative expression
F
iNOS/Arginase
IL-4
G
Relative expression
H
Relative expression

Once the polarization states of the macrophages were validated, the rate of choline uptake was examined. After being polarized, the rate of uptake of radiolabeled ^{3}H-choline was measured at time points over a 30 minute interval (Figure 5). Choline uptake was increased under both classical and alternative activated conditions, with a significant increase in uptake at both the 20 and 30 minute time periods.

The kinetics of choline uptake were also measured following macrophage polarization (Figure 6). Classical activation decreased the K_m from 93.30 μM to 57.78 μM and increased the V_{max} from 7.945 pmol/mg/min to 15.40 pmol/mg/min (Table 1). Alternative activation similarly altered the V_{max}, increasing it to 16.78 pmol/mg/min, although the K_m did not significantly change relative to control conditions. Both the rate and kinetic analysis of choline uptake show an increase in choline transport in polarized macrophages relative to their unstimulated counterparts.

Figure 5. Effect of macrophage polarization on the rate of choline uptake.

Wild-type BMDM were treated with LPS (100 ng/mL, A in red) or IL-4 (20 ng/mL, B in blue) for 48 hours prior to measuring choline uptake. Choline uptake was measured relative to untreated control (black) over respective time intervals by incubating cells in a solution of KRH buffer containing 1 μCi/mL of ^{3}H-choline chloride. Choline uptake was determined by measuring presence of the radiolabel in the cell lysate following uptake experiment. Statistical significance determined using Sidak's multiple comparisons from a two way ANOVA (n=4-6, * $p<0.05$, ** $p<0.01$). A significant increase in uptake was observed in response to both LPS ($p<0.0001$, DF = 7, F = 42.71) and IL-4 ($p<0.0001$, DF = 7, F = 13.88).

A

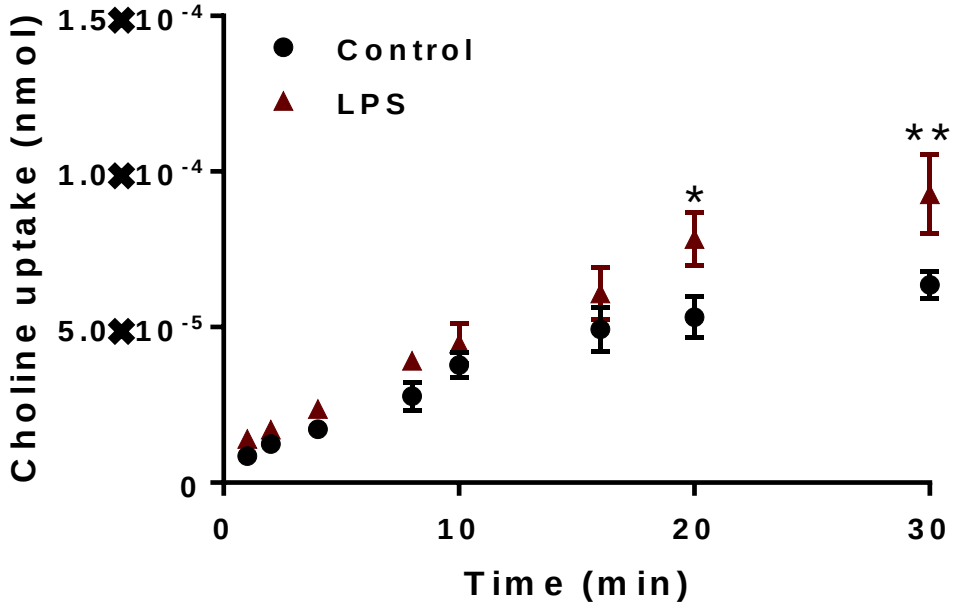
Choline uptake (nmol)
1.5✖10 -4
1.0✖10 -4
5.0✖10 -5
0
Control
LPS
*
**
0
10
20
30
Time (min)

B

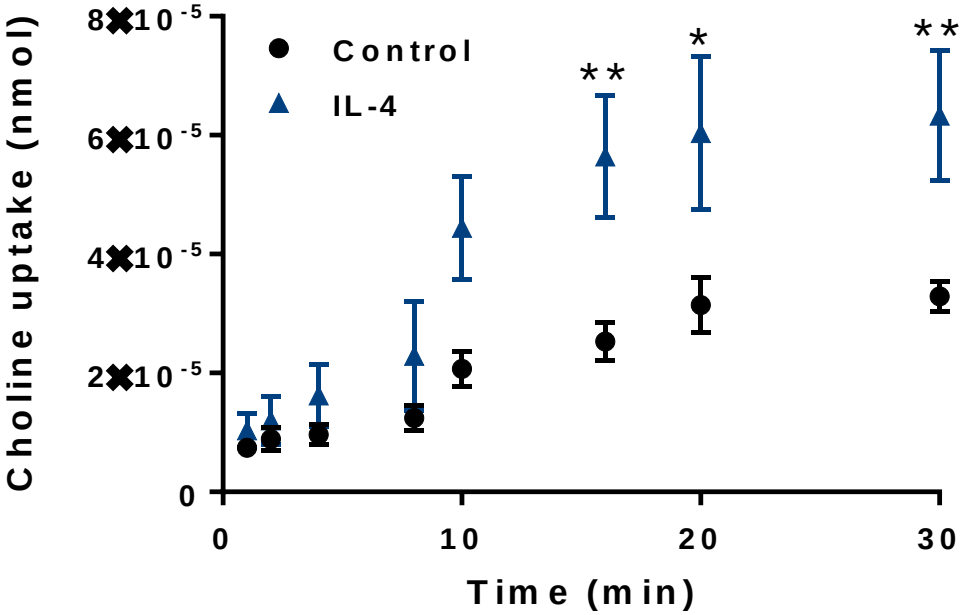
Choline uptake (nmol)
8✖10 -5
6✖10 -5
4✖10 -5
2✖10 -5
0
Control
IL-4
**
*
**
0
10
20
30
Time (min)

Figure 6. Effect of macrophage polarization on the kinetics of choline transport.

Wild-type BMDM were treated with LPS (100 ng/mL, A) or IL-4 (20 ng/mL, B) for 48 hours prior to measuring choline uptake. Choline uptake was measured over ten minutes by incubating cells in a solution of KRH buffer containing 1μCi/mL of ^{3}H-choline chloride. Michaelis-Menten constants were determined using Graphpad Prism 6 non-linear regression analysis and are shown in Table 1 (n=4-6).

A

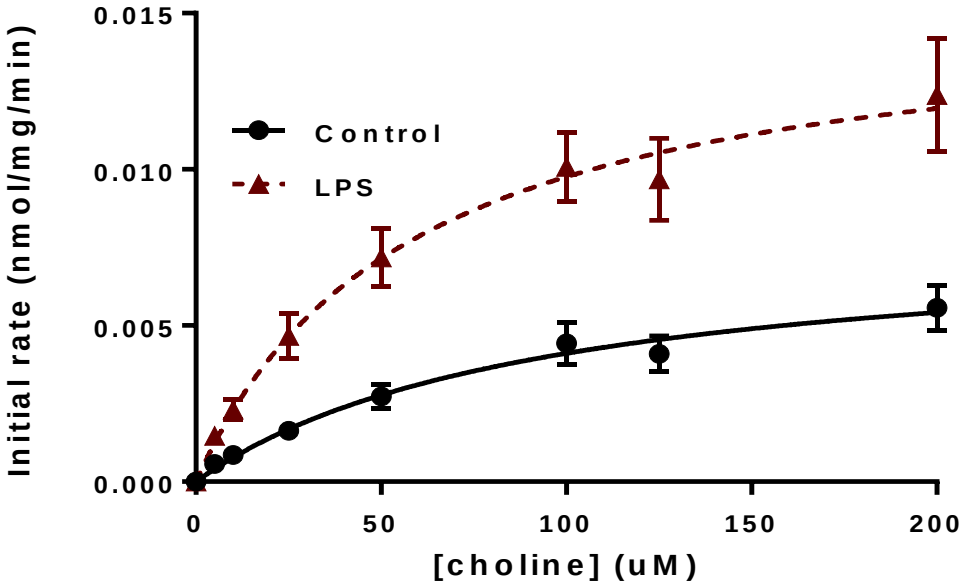
0.015
0.010
0.005
0.000
Initial rate (nmol/mg/min)
Control
LPS
0
50
100
150
200
[choline] (uM)

B

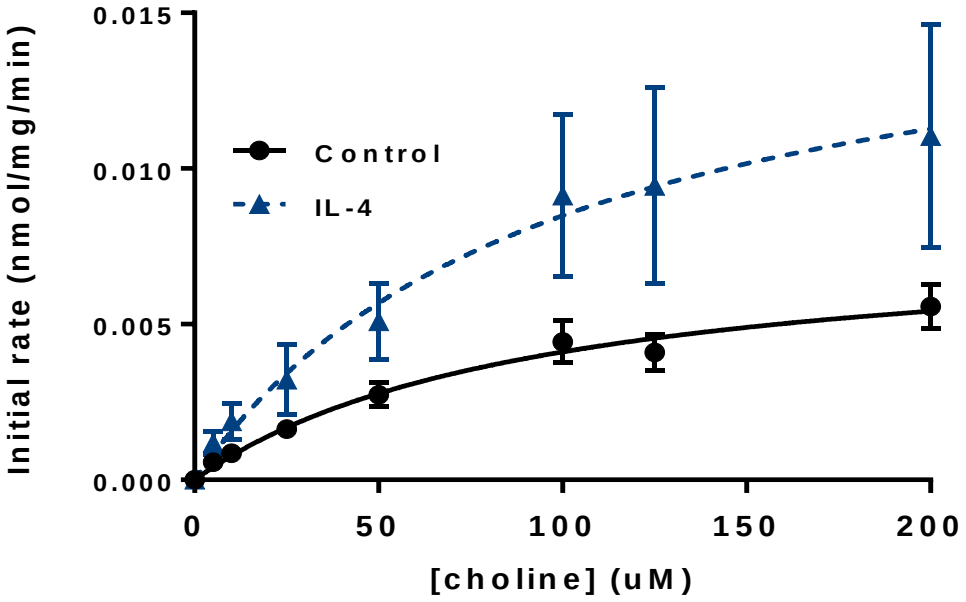
0.015
0.010
0.005
0.000
Initial rate (nmol/mg/min)
Control
IL-4
0
50
100
150
200
[choline] (uM)

Table 1. Michaelis-Menten values for choline uptake in stimulated macrophages

Treatment	K_m (μM)	V_{max} (pmol/mg/min)
Control	93.30 ± 34.43	7.945 ± 1.340
LPS	57.78 ± 18.54	15.40 ± 1.87
IL-4	97.71 ± 75.71	16.78 ± 6.048

The final choline uptake experiment that was performed tested BMDM sensitivity to HC-3, a choline uptake inhibitor that prevents choline-specific transport. IC_{50} values for HC-3 did not change in response to macrophage polarization relative to untreated controls (Figure 7). Altogether, choline uptake studies following macrophage polarization revealed the rate and kinetics of choline uptake were increased in response to both classical and alternative activation, and that choline specific transport mechanisms remained responsible for the choline uptake under polarized conditions.

Since most of choline's metabolic functions are due to its incorporation into PC, it was next investigated whether macrophage polarization influences choline's incorporation into lipids (Figure 8). Both classical and alternative stimulation increased choline incorporation across all time points, with significant increases in choline incorporation occurring after 8 hours in LPS stimulated cells and at 4, 6, and 8 hours in IL-4 stimulated cells. These experimental findings confirm that the change in choline uptake in response to macrophage polarization is also observed at the PC level.

Figure 7. Effect of macrophage polarization HC-3 sensitivity.

Wild-type BMDM were treated with LPS (100 ng/mL) or IL-4 (20 ng/mL) for 48 hours prior to measuring choline uptake (control shown in black). Choline uptake was measured over ten minutes by incubating cells in a solution of KRH buffer containing 1μCi/mL of ^{3}H-choline chloride containing various concentrations of HC-3. IC_{50} curves were fit with GraphPad Prism 6 non-linear regression analysis. Values for HC-3 IC_{50} are 141.1 μM for control, 170.4 μM for LPS, and 124.8 μM for IL-4 (n= 4-6).

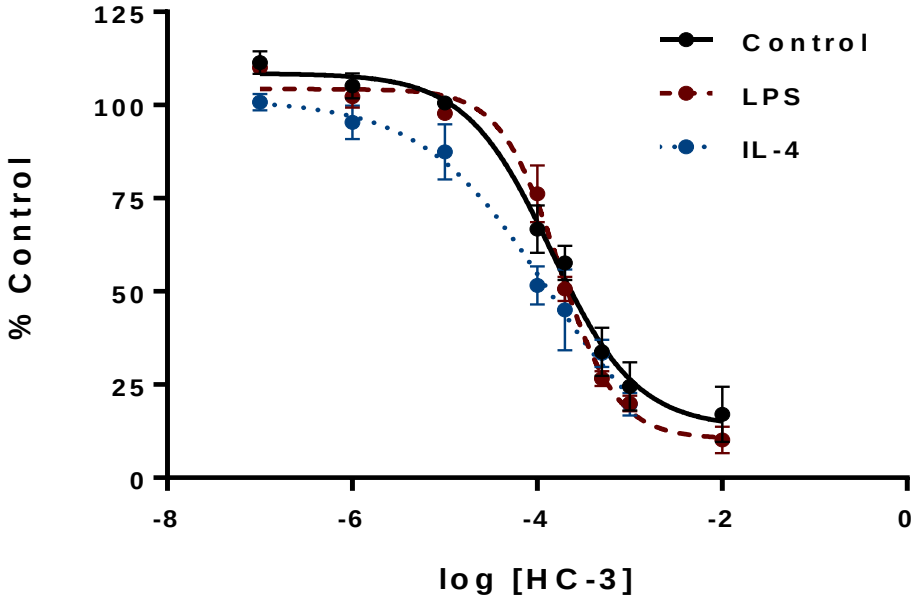
125
100
75
50
25
0
% Control
-8
-6
-4
-2
0
log [HC-3]
Control
LPS
IL-4

Figure 8. Effect of macrophage polarization on choline incorporation into lipids.

Wild-type BMDM were treated with LPS (A in red) or IL-4 (B in blue) for 48 hours (control shown in black). Following the 48 hour incubation, cells were incubated in media containing 1μCi/mL of ^{3}H-choline chloride for respective time interval. Cell were lysed with a freeze-thaw cycle and a lipid extraction was performed. Choline incorporation was determined by measuring the presence of the ^{3}H-choline radiolabel in the lipid phase. Statistical analysis was performed using Sidak's multiple comparison's test on a two-way ANOVA (n= 6; ** $p<0.01$, **** $p<0.0001$). A significant increase in uptake was observed in response to both LPS ($p<0.0001$, DF = 7, F = 23.78) and IL-4 ($p<0.0001$, DF = 7, F = 22.49).

A

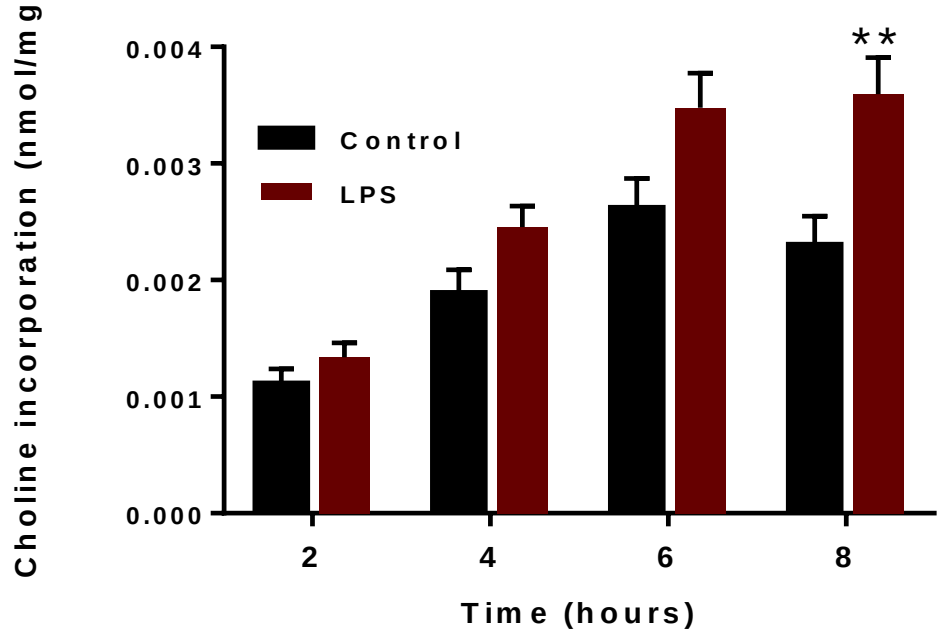
Choline incorporation (nmol/mg)
0.004
0.003
0.002
0.001
0.000
Control
LPS
**
2
4
6
8
Time (hours)

B

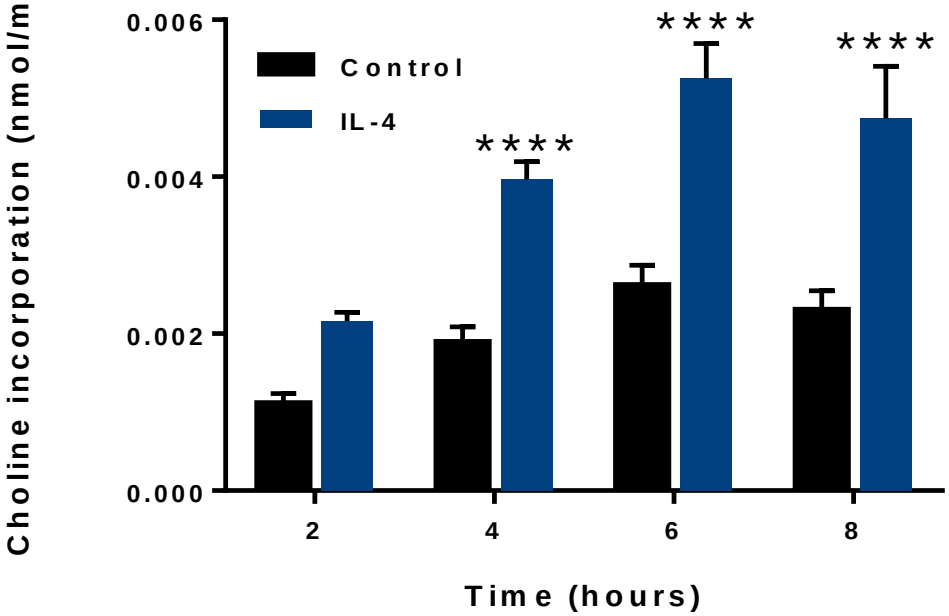
Choline incorporation (nmol/mg)
0.006
0.004
0.002
0.000
Control
IL-4
****
****
****
2
4
6
8
Time (hours)

6.2 Macrophage polarization increases CTL1 expression

With the substantial increase in choline uptake and PC incorporation observed in response to macrophage polarization, it was hypothesized that CTL1, the most widely expressed choline transporter may facilitate the observed increase in uptake. To investigate this hypothesis, RNA (Figure 9A CTL1, 9B CTL2) and protein expression (Figure 9C/D) were measured following the macrophage polarization induced in the choline metabolism experiments. Among all the choline transporters probed using qPCR (CTL1-5, OCT1-4, CHT1), CTL1 and CTL2 were the only transporters expressed in BMDM. In response to chronic classical activation, CTL1 expression at the mRNA and protein level was significantly increased compared to untreated cells. CTL2 expression was increased at the RNA level following LPS induction, although its protein expression was not measured. Alternative activation induced an increase in CTL1 protein expression, although RNA expression remained similar to control levels. CTL2 transcript expression did not change in response to IL-4. These results suggest CTL1 may facilitate the increase in choline metabolism fueled by inflammatory stimulation.

Figure 9. LPS treatment increases CTL1 and CTL2 expression.

Wild-type BMDM were treated with LPS (100 ng/mL, red) or IL-4 (20 ng/mL, blue) for 48 hours. RNA expression was measured for CTL1 (A) and CTL2 (B) and was set relative to untreated control using the delta delta Ct method. Statistical significance was measured using a one-way ANOVA (n= 3; $p<0.0001$, $F= 47.77$). Multiple comparisons were performed using Dunnet's test (*** $p<0.001$, **** $p<0.0001$). Other choline transporters were not expressed in BMDM (CTL3-5, OCT1-3, CHT1). Western Blot was performed on an 8% SDS-PAGE gel (C) and standardized to a β-actin internal control (Densitometry results shown in D). Statistical significance was measured using a one-way ANOVA (n= 3; $p<0.05$, $F= 6.199$). Multiple comparisons were performed using Dunnet's test ANOVA (n=3; * $p<0.05$, *** $p<0.001$, **** $p<0.0001$).

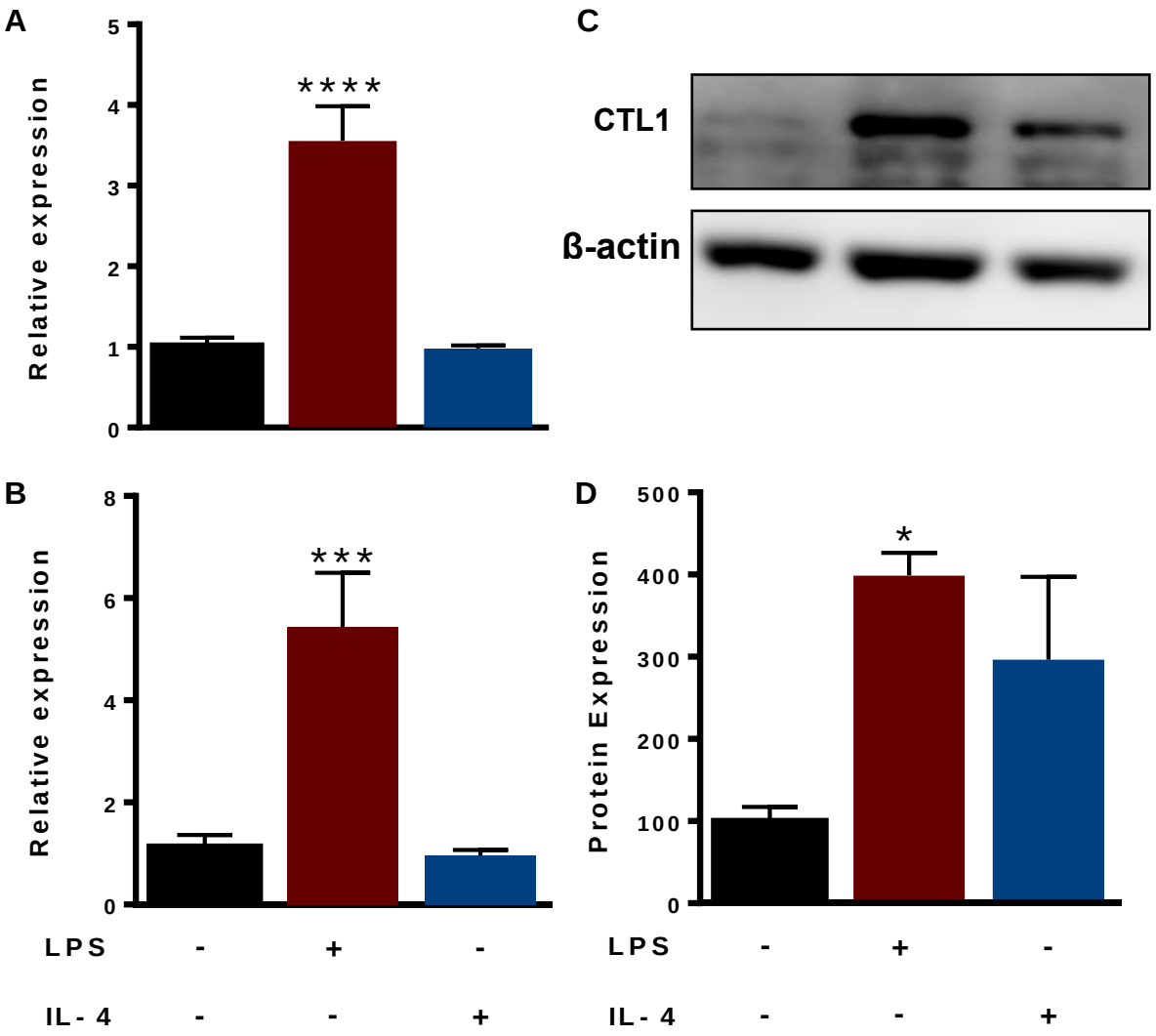
A
Relative expression
5
4
3
2
1
0
****
C
CTL1
ß-actin
B
Relative expression
8
6
4
2
0
***
D
Protein Expression
500
400
300
200
100
0
*
LPS - + - LPS - + -
IL-4 - - + IL-4 - - +

6.3 CTL1 drives choline metabolism in BMDM

Although CTL1 and CTL2 were the only choline transporters detected in BMDM, their relative contributions to choline transport are unknown. In order to isolate the effects of CTL1 on choline metabolism, a $CTL1^{-/-}$ mouse was generated by knocking out exon 3 of the CTL1 gene. The excision of exon 3 was confirmed by the appearance of a knockout DNA fragment and the disappearance of the wild-type CTL1 band in $CTL1^{-/-}$ mice (Figure 11). Exon 3 deletion substantially reduced CTL1 mRNA levels compared to littermate wild-type controls (Figure 11A). Choline metabolism was also evaluated by looking at ^{3}H-choline uptake over ten minutes and ^{3}H-choline incorporation into lipids over 48 hours. CTL1 deficient mice showed a marked reduction in choline uptake (11B) and choline incorporation into lipids (Figure 11C) relative to their wild-type controls. The reduced choline metabolism observed in $CTL1^{-/-}$mice suggests that CTL1 is not only necessary for choline uptake but it is required for PC synthesis in BMDM.

Figure 10. Breeding and genotyping of CTL1$^{-/-}$ mice.

(A) A female Cre positive mouse was bred with a male CTL1 floxed mouse (fl). This cross is denoted as the F_0 generation. Females from the F_0 cross were bred with male mice with two copies of the floxed CTL1 allele. Males from the F_0 cross were bred with female mice with two copies of the floxed CTL1 allele. These crosses yielded CTL1$^{-/-}$ mice. (B) Genotyping results from the F1 pairings described above, with the CTL1$^{-/-}$ mice highlighted in the red boxes (wild-type; WT).

A

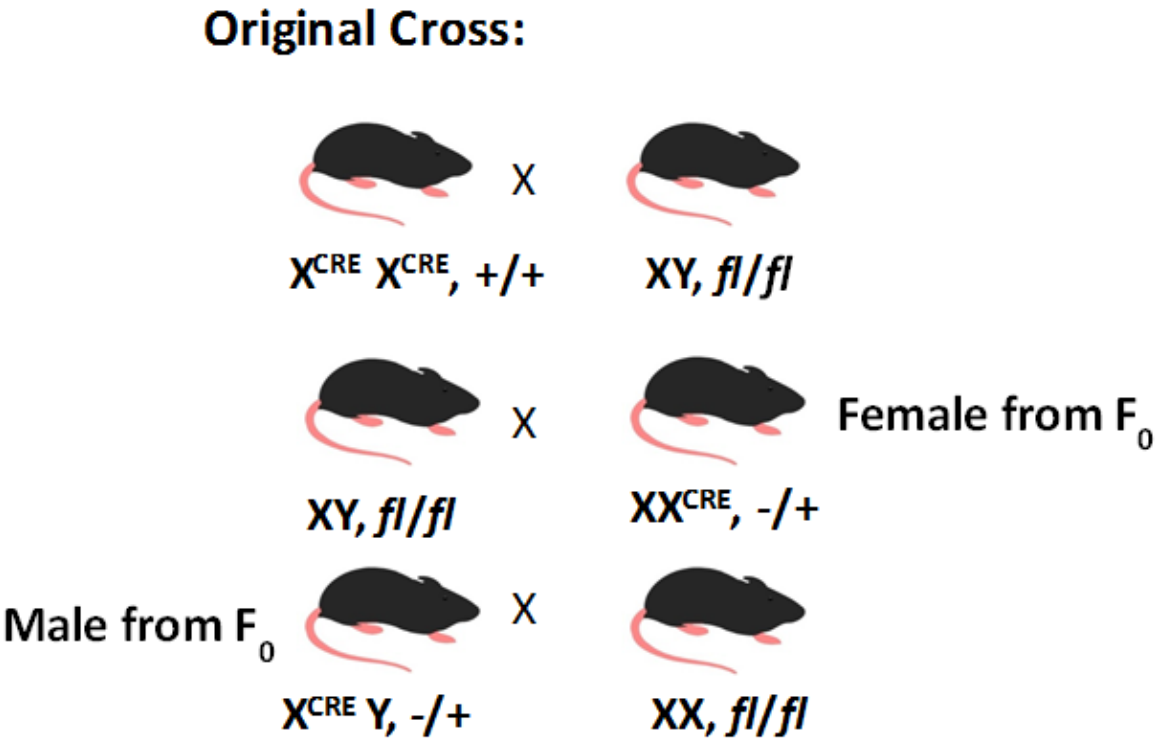
Original Cross:
X
X^{CRE} X^{CRE}, +/+
XY, *fl/fl*
X
XY, *fl/fl*
Female from F_0
XX^{CRE}, -/+
Male from F_0
X
X^{CRE} Y, -/+
XX, *fl/fl*

B

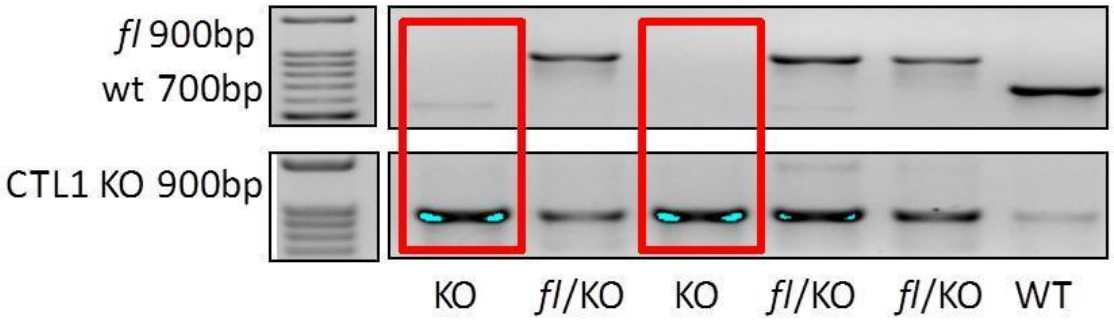
fl 900bp
wt 700bp
CTL1 KO 900bp
KO
fl/KO
KO
fl/KO
fl/KO
WT

Figure 11. CTL1 knockout in BMDM reduces choline uptake and metabolism.

In BMDM derived from CTL1 KO mouse, CTL1 mRNA expression was decreased (A). Choline uptake (B) was measured over ten minutes by incubating cells in a solution of KRH buffer containing 1μCi/mL of ^{3}H-choline chloride. Incorporation of ^{3}H-choline chloride into the lipid phase was also measured over 48 hours (C). Choline uptake and incorporation were both reduced in the CTL1 KO relative to wild-type cells (n=2).

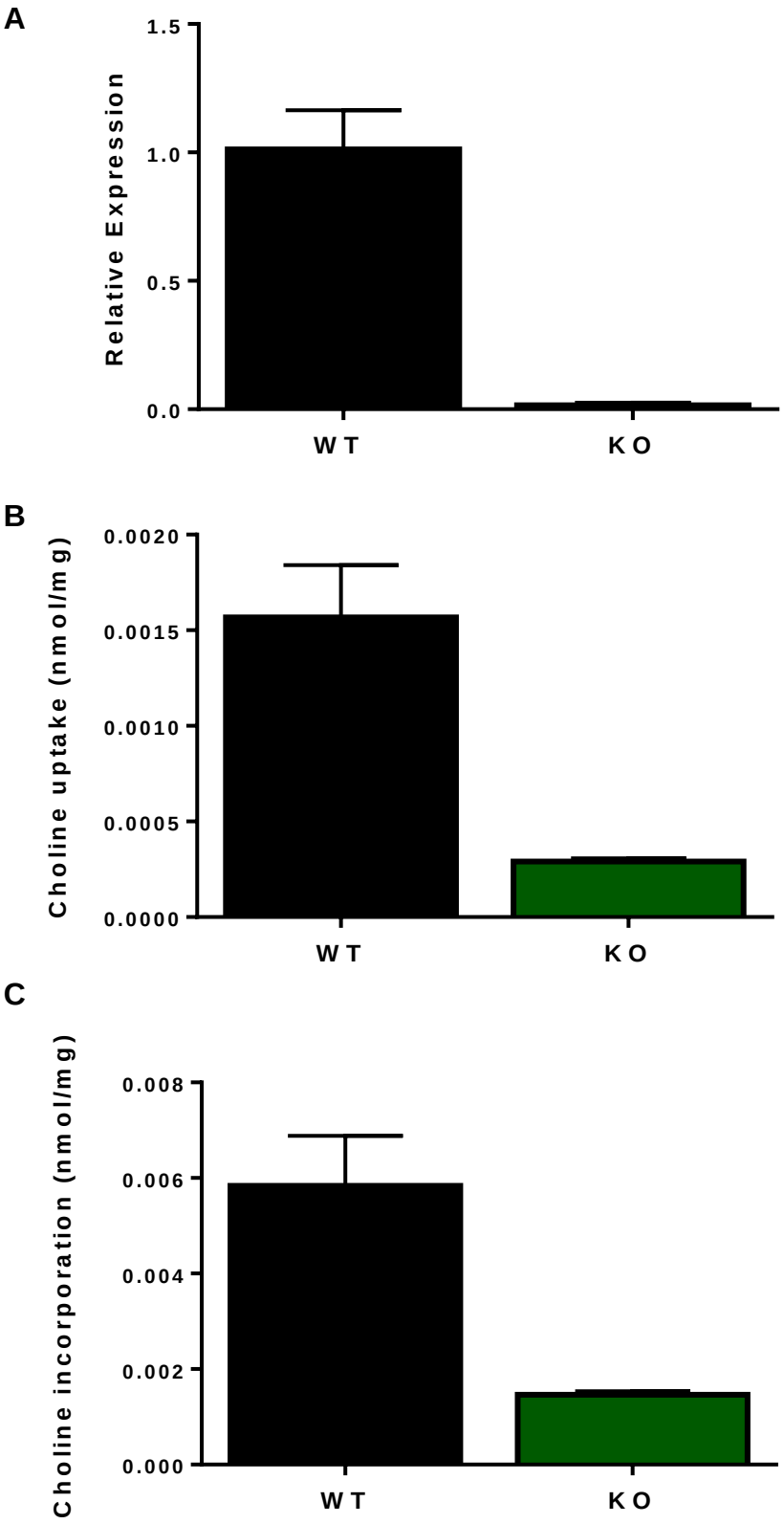
A
Relative Expression
1.5
1.0
0.5
0.0
WT
KO
B
Choline uptake (nmol/mg)
0.0020
0.0015
0.0010
0.0005
0.0000
WT
KO
C
Choline incorporation (nmol/mg)
0.008
0.006
0.004
0.002
0.000
WT
KO

6.4 Choline depletion alters LPS-induced cytokine secretion

The second objective of my research was to investigate the effect of choline depletion on cytokine secretion. Two different methods were used to induce choline depletion in wild-type BMDM: pharmacological inhibition using choline uptake inhibitors, and antibody occlusion using CTL1 antibodies. HC-3 reduced acute choline uptake below 20% of control levels, while DMAE reduced uptake below 5% of control levels (Figure 12A). This change was also observed at the lipid level, with choline's incorporation into lipids reduced to approximately 60% of control levels in HC-3 treated samples and to approximately 25% of control levels with DMAE treatment (Figure 12B). Antibody occlusion was performed using C-terminal and N-terminal CTL1 antibodies obtained from Dr. Marica Bakovic's group at the University of Guelph (see methods for specifications). An IgG control was also used to eliminate any non-specific effects. Antibody occlusion at both the N-terminal and C-terminal end of CTL1 facilitated choline depletion, with N-terminal occlusion exhibiting more drastic effects. C-terminal antibody treatment reduced choline uptake to below 50% of the untreated control, with the N-terminal antibody reducing choline uptake below 20% of control levels (Figure 12C). Similar effects were observed examining choline's incorporation into lipids, with the C-terminal and N-terminal antibodies reducing choline incorporation to roughly 58% and 22% of control levels respectively (Figure 12D). The results from both choline uptake inhibitor and the antibody treatments validate their ability to induce choline deficiency in BMDM.

Figure 12. Choline uptake inhibitors and CTL1 antibody treatment decrease choline uptake and incorporation into lipids.

Effect of pharmacological inhibition with choline uptake inhibitors HC-3 and DMAE on choline uptake (A) and incorporation into lipids (B) was measured using radiolabeled ^{3}H-choline chloride (1μCi/mL). Uptake was measured over ten minutes in the presence of either HC-3 (250 μM), DMAE (500 μM), or a vehicle control while incorporation was measured over 48 hours in the presence of the inhibitors. Choline uptake was determined by measuring the presence of the ^{3}H radiolabel in the cell lysate. Statistical analysis was performed using a one way ANOVA (n= 4; $p<0.01$ and F= 8.076 for incorporation, $p<0.001$ and F= 19.67). Multiple comparisons were performed using Dunnett's test (** $p<0.01$, **** $p<0.0001$). Effect of CTL1 antibody occlusion on choline uptake (C) and incorporation (D) was also measured. Antibody treatments (1/100 dilution of stock) were applied for 1 hour prior to uptake and applied during incubation with the radiolabel. Choline incorporation was determined by measuring the presence of the ^{3}H radiolabel in the lipid phase following a lipid extraction. Statistical analysis was performed using a one way ANOVA (n= 4; $p<0.01$ and F= 10.74 for incorporation, $p<0.001$ and F= 13.57). Multiple comparisons were performed using Dunnett's test (* $p<0.05$, ** $p<0.01$, **** $p<0.0001$).

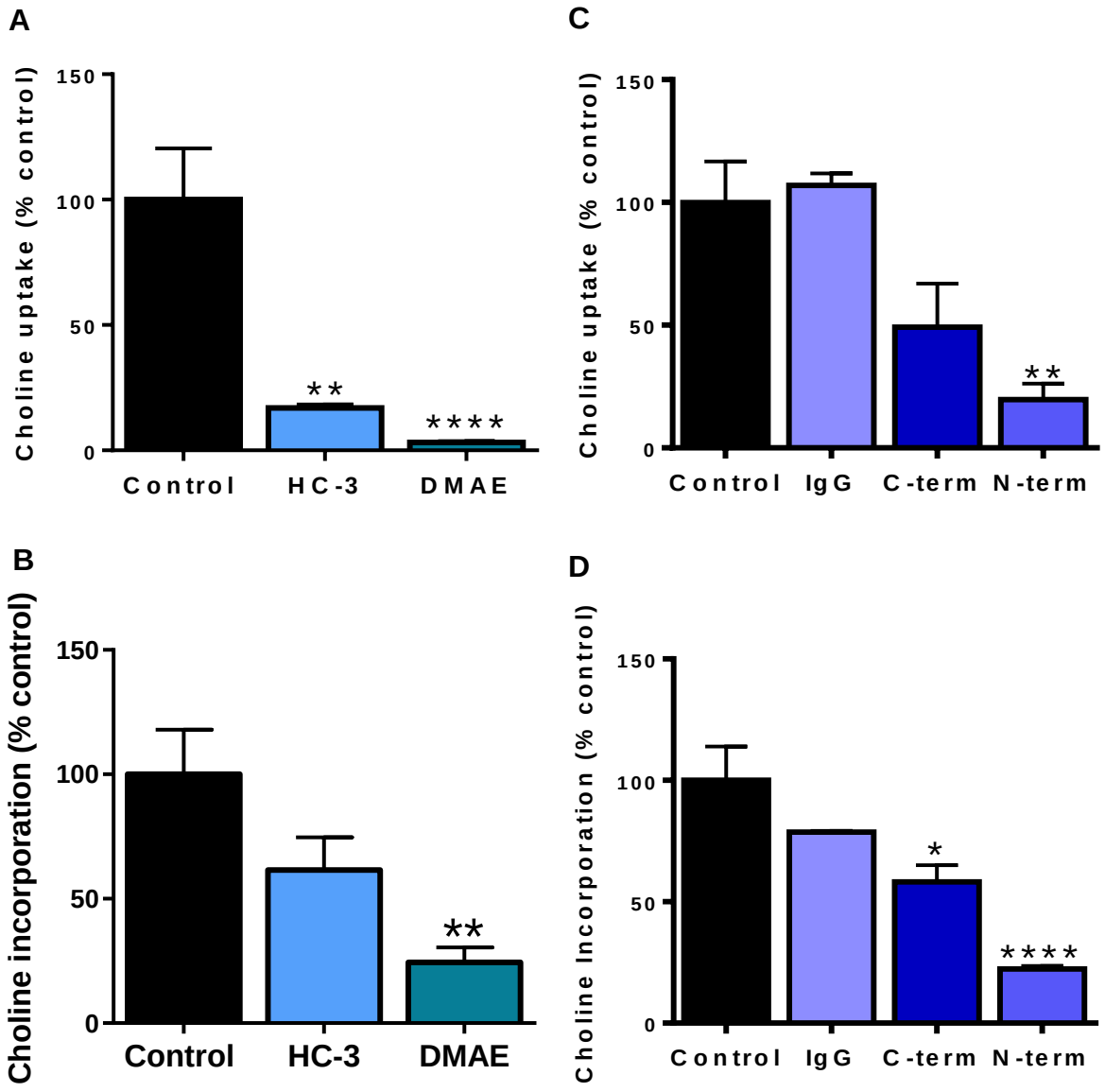
A
Choline uptake (% control)
150
100
50
0
**
****
Control
HC-3
DMAE
C
Choline uptake (% control)
150
100
50
0
**
Control
IgG
C-term
N-term
B
Choline incorporation (% control)
150
100
50
0
**
Control
HC-3
DMAE
D
Choline Incorporation (% control)
150
100
50
0
*
****
Control
IgG
C-term
N-term

Following their validation, both methods of choline depletion were used to measure the effects of choline depletion on cytokine secretion. For the antibody occlusion experiment, only the C-terminal CTL1 antibody was used due N-terminal antibody occlusion significantly reducing total protein, therefore possibly effecting cell viability. Choline deficiency increased the secretion of TNF-α across all choline depleted treatments relative to control LPS treated cells (Figure 13A). DMAE and HC-3 both showed considerable increases in TNF-α secretion, while C-terminal antibody treatment showed a modest increase relative to wild-type. IL-10 secretion was also altered following choline depletion (Figure 13B). HC-3 and C-terminal antibody treatment reduced IL-10 secretion; while DMAE induced choline deficiency increased cytokine secretion. IL-6 secretion was not significantly different from LPS treated control cells in response to choline depletion via the choline uptake inhibitors DMAE and HC-3 (Figure 13C). However, CTL1 occlusion using the C-terminal antibody showed a significant decrease in IL-6 secretion. IL-1β secretion was also measured; however no response to LPS was observed (data not shown). These results indicate that choline depletion alters cytokine secretion and differentially alters pro-inflammatory and anti-inflammatory cytokines.

Figure 13. Effect of choline depletion on cytokine secretion.

BMDM were choline depleted for 48 hours by either treating with choline uptake inhibitors (HC-3 – 250 μM, DMAE - 500 μM) or by incubating with a C-terminal CTL1 antibody (refer to Methods for specific antibody information). Following choline depletion cells were treated with 100 ng/mL LPS for 6 hours. Concentrations of TNF α (A), IL-10 (B), and IL-6 (C) in the media were measured using R&D systems Duoset ELISA kits. Statistical analysis was performed using Dunnet's multiple comparison's test on a one way ANOVA (n= 3-11; ** $p<0.01$).

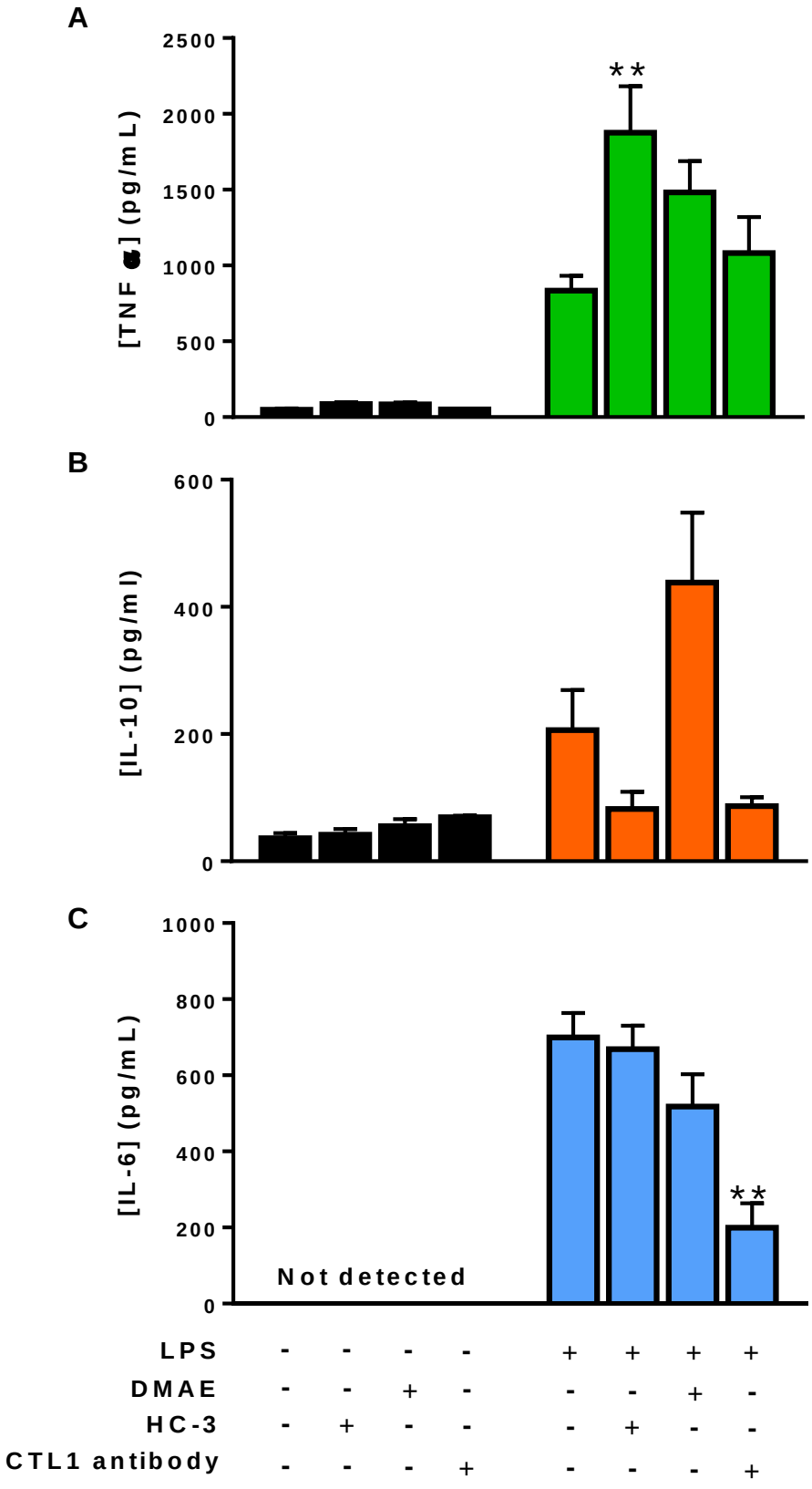
A
2500
2000
1500
1000
500
0
**
[TNF α] (pg/mL)
B
600
400
200
0
[IL-10] (pg/ml)
C
1000
800
600
400
200
0
**
Not detected
[IL-6] (pg/mL)
LPS - - - - + + + +
DMAE - - + - - - + -
HC-3 - + - - - + - -
CTL1 antibody - - - + - - - +

7.0 DISCUSSION

As an innate immune cell that acts as one of the first lines of defense against pathogenic infection, macrophages play a pivotal role in regulating host cell immunity. With recent evidence implicating the metabolic status of cells as key mediators in the regulation of the inflammatory response, this study looked to investigate the link between choline metabolism and inflammation (Galvan-Pena and O'Neill, 2014; Peyssonnaux et al., 2005; Tian et al., 2008)
.

During my initial attempts to determine the relationship between choline metabolism and inflammation, I examined choline uptake in RAW 264.7 macrophages (Supplementary Figure 6). As an immortalized cell line, RAW 264.7 macrophages provided the ability to conduct higher throughput experiments and the potential for genetic manipulation, making them advantageous over primary cells. However, their rapid proliferation made it difficult to standardize biological replicates and potentially masked effects of polarization on choline metabolism due to a naturally high requirement for PC. Also, the development of the $CTL1^{-/-}$ mouse provides a better model for the study of CTL1 knockout, eliminating the benefits of the genetic manipulation of RAW 264.7. For these reasons, the cell line for my research from RAW 264.7 cells to primary BMDMs.

7.1 Macrophage polarization increases choline uptake and metabolism

Although it had been established that acute LPS induction increases the incorporation of choline into PC, the influence IL-4 on choline incorporation and the effect of polarization on choline uptake was unknown. In this study, IL-4 stimulation caused an increase in choline incorporation into PC, while LPS exhibited similar effects on choline incorporation as

described previously (Fig 8). The observed increase in the rate of choline uptake when macrophages are both classically and alternatively polarized suggests that the increase in incorporation into PC is facilitated by an increase in choline uptake (Figure 5). No change in HC-3 sensitivity suggests that the type of transporter responsible for choline transport remains unchanged following macrophage polarization (Figure 7).

The observed change in choline metabolism appears to be driven by changes in transport kinetics which is supported by the Michaelis-Menten curves (Figure 6). Both LPS and IL-4 increase the apparent V_{max} of choline transport, however each has a different impact on the apparent K_m, with LPS decreasing the apparent K_m and IL-4's K_m remaining unchanged. The difference in K_m values measured may be due to the fit of the IL-4 Michaelis-Menten curve. Due to the high standard error and the limited amount of points on the curve, the K_m value is volatile. Repetition of the IL-4 induced choline kinetic experiments will help reduce the standard error and provide a better fit to determine whether the observed difference between LPS and IL-4 stimulated conditions were real or erroneous. Despite the different K_m values under LPS and IL-4 stimulated conditions, both macrophage polarization states show an increased capacity to take up choline. One possible explanation for could be an increase in the biosynthetic flux through the Kennedy pathway. Although there is limited data surrounding IL-4's effect on the enzymes of the CDP-choline pathway, previous findings have shown LPS increased the expression of both CCT and CPT, the final two enzymes in the Kennedy pathway. In B cells, LPS increased the transcription of CPT and decreased CCT degradation in response to LPS (Fagone et al., 2007). Another study performed in macrophages revealed increased expression of both CPT and CCT under LPS stimulated conditions (Tian et al., 2008). The findings in these studies prove that Kennedy pathway enzymes respond to

inflammation, providing a possible mechanism for the observed increase in choline metabolism.

7.2 Increased CTL1 expression may facilitate increased choline metabolism following macrophage polarization

Although Kennedy pathway enzymes are increased in response to LPS, which could explain the increase in uptake observed in the rate and kinetic analyses, previous research has shown that $CCT^{-/-}$ mouse are still able to increase choline metabolism when challenged with LPS. This may suggest that multiple mechanisms facilitate increased choline uptake in polarized macrophages. Another possible mechanism inflammation could mediate increased choline metabolism is by increasing the expression of choline transporter. Since choline-like transporters mediate the majority of choline transport in BMDM, I next investigated whether CTL1 and CTL2 expression change in response to inflammation. Following macrophage polarization, LPS increased mRNA and protein expression of CTL1, while IL-4 increased the amount of CTL1 protein. This suggests LPS induces increased CTL1 through transcriptional activation whereas IL-4 increases CTL1 levels post-transcriptionally. In the initial characterization of the CTL1 promoter, it was discovered that CTL1 contained a binding site for NFκB, which was validated by gel mobility shift assays (Yuan et al., 2006). This binding sight may provide a mechanism for increased CTL1 expression in response to LPS induction. Although an increase in total CTL1 protein provides a logical explanation for the observed increase in choline uptake, flow cytometry experiments be needed to demonstrate that increases in CTL1 protein induced by LPS and IL-4 alters the surface expression of CTL1.

These results are at odds with the disappearance of CTL1 from the cell surface of THP-1 monocytes-derived macrophages (Fullerton et al., 2006). However, THP-1 macrophages are

induced with phorbol ester treatment, which could interfere with normal cellular expression. Also, the comparison of human and mouse cells adds a level of complexity that warrants further consideration. In addition, the CTL1$^{-/-}$ mouse provides an additional means to test CTL1's role in facilitating an inflammatory mediated increase in choline metabolism. Observing no increase in choline uptake in response to macrophage polarization in CTL1$^{-/-}$ BMDM could provide conclusive evidence that CTL1 causes this inflammatory mediated response.

7.3 Increased choline uptake may accommodate increased protein trafficking

Increased choline uptake and metabolism independent of the nature of inflammatory stimulus may suggest that PC is necessary to accommodate an increased burden of secreting and trafficking inflammatory proteins. Cytokines are trafficked from the endoplasmic reticulum through the trans Golgi network (TGN) in response to LPS much in the same way proteins are trafficked intracellularly (Manderson et al., 2007; Murray and Stow, 2014). Several studies have associated a reduction of PC levels with ER and Golgi dysfunction. The Chinese hamster ovary cell line MT58 provides an excellent model to study PC depletion due to a thermosensitive mutation in their CCT gene. At the restrictive temperature which induces CCT inactivity and PC depletion, an increase in CCAAT/enhancer-binding protein homologous protein (CHOP) is observed (van der Sanden et al., 2003). CHOP is a transcription factor that is activated by the unfolded protein response triggered by ER stress and can lead to apoptotic cell death (Marciniak et al., 2004; Nishitoh, 2012). Apoptosis in MT58 cells is rescued by lyso-PC treatment, suggesting PC may be the trigger to ER stress induced apoptosis (van der Sanden et al., 2003). In a separate study involving the same thermosensitive cell line, ER and Golgi structure and function was examined under thermorestrictive conditions. PC

depletion led to structural abnormalities in the ER, with the appearance of spherical like ER structures rather than its normal tubular like structure (Testerink et al., 2009). Normal ER structure was observed upon PC rescue with lyso-PC treatment (Testerink et al., 2009). No structural abnormalities were observed in the Golgi; however PC depletion did cause a reduction of protein secretion through the Golgi body, which was also rescued with lyso-PC treatment (Testerink et al., 2009). These studies support that PC may play a role in ER and Golgi dysfunction and reduction of PC could alter protein trafficking though the TGN, thus also affecting cytokine release. Similar defects in protein trafficking are observed in cytokine secretion in macrophages lacking CCTα. Inhibition of *de novo* PC synthesis reduced the secretion of TNF and IL-6 into the media. Fluorescently tagged proteins revealed that both TNF and IL-6 aggregated intracellularly in CCTα deficient cells following LPS stimulation while wild-type cells showed efficient release of both cytokines. Lyso-PC treatment restored normal TNF secretion (Tsao et al., 2014).

7.4 Choline deficient conditions promote pro-inflammatory state

Both the CCTα knockout experiments and the MT58 thermosensitive CCTα experiments suggest that increased choline uptake could help provide additional PC which supports normal protein trafficking that is important to the inflammatory response in both classically and alternatively activated macrophages. This theory is supported by the choline depleted cytokine secretion experiments above, which reveal altered cytokine secretion under choline deficient conditions (Figure 13). Each treatment to induce choline deficiency had differing effects on cytokine secretion. HC-3, which is a competitive inhibitor of choline transport, increased TNF-α secretion, decreased IL-10 secretion, but did not change IL-6 secretion. HC-3's ability to augment the secretion of TNF-α suggests that inducing choline

deficiency by inhibiting choline uptake with HC-3 is not sufficient to significantly inhibit protein trafficking and is counter to previous results from CCTα null macrophages (Tian et al., 2008). This is further supported by the CTL1 antibody and DMAE data, which both show increased TNF-α secretion relative to untreated cells (Figure 13A). Intact protein trafficking may be in place due to compensatory effects of other PC metabolic pathways. During choline deficiency induced by CCT inactivity, exogenous lysophosphatidylcholine is capable of rescuing cells, indicating the Lands pathway may be able to provide sufficient levels of PC (Esko et al., 1982). Further increased fatty acid remodeling is observed during CCT deficiency, which could be indicative of increased Lands cycle activity (Caviglia et al., 2004). Experiments specifically examining total PC content will complement the chronic radiolabeling experiments used here to assess PC levels.

In both the HC-3 and CTL1 occluded treatments, macrophages showed increased secretion of TNF-α and decreased secretion of IL-10. DMAE showed an increase in TNF-α as observed with the other treatments, but also showed an increase in IL-10 secretion. The results in the DMAE trials were quite divergent between biological replicates and require further repetition before significant conclusions can be made on the data. As a means to rescue the competitive inhibition of HC-3, experiments could use an excess of choline in the presence of the inhibitor. In this case choline supplementation may attenuate the increase in TNFα, assuming that the excess of choline in isolation did not have adverse effects.

The increased TNF-α and decreased IL-10 secretion may be indicative of a shift in polarization state of the cells towards a more pro-inflammatory phenotype. In a whole body context, such a shift could have a negative effect on immunometabolic outcomes. Pro-inflammatory signaling can increase macrophage localization to adipose tissue and increase

adipose tissue inflammation (Gao et al., 2002; Hotamisligil et al., 1993; Weisberg et al., 2003). Pro-inflammatory signaling can also directly impact insulin signaling, with NF-κB activation leading to the phosphorylation and inactivation of insulin receptor substrates (Gao et al., 2002; Ueki et al., 2004). The inflammatory profile observed the choline deficient model generated through HC-3 and CTL1 occlusion has the potential to initiate a similar metabolic response, which leaves the possibility that choline availability alter the progression of metabolic disease.

7.5 Possible mechanisms of altered cytokine secretion under choline deficient conditions

Certain disturbances to lipid metabolism that may occur under choline deficient conditions could explain the alteration to the macrophage inflammatory profile in response to LPS. Sphingomyelin, a sphingolipid embedded in the plasma membrane, can be broken down into ceramide and phosphocholine by phospholipase C. Choline deficiency has been shown to decrease sphingomyelin and increase ceramide levels intracellularly (Yen et al., 1999). Under normal cellular conditions, this lipid signaling pathway helps initiate apoptosis through NF-κB activation, which could initiate a pro-inflammatory response (Schutze et al., 1992). Another possible mechanism for altered inflammatory signaling mediated by choline deficiency could be increased concentrations of DAG. Under choline deficient conditions, inadequate CDP-choline concentrations leads to an accumulation of diacylglycerol (Yen et al., 1999). DAG is a potent activator of protein kinase C (PKC), which increases signal transduction through the NF-κB pathway (Asehnoune et al., 2005; Zhou et al., 2006). In addition, treatment of macrophages with a PKC inhibitor reduces LPS-induced inflammatory signaling (Asehnoune et al., 2005; Zhou et al., 2006). An accumulation of DAG under choline deficient conditions could potentially lead to PKC activation and increased signal transduction through the TLR4 pathway, causing an increase in pro-inflammatory signaling. Future work

should aim to specifically measure lipid species (sphingomyelin, ceramide, and DAG) to determine the potential influence of these pathways.

Although increased NF-κB activation by ceramide signaling or PKC activation could be the underlying mechanism causing altered cytokine secretion under choline deficient conditions, it cannot exclusively account for the differential secretion of TNF-α and IL-10. Also, IL-6 secretion was significantly inhibited in CTL1 antibody treated samples but not in HC-3 or DMAE treated samples. IL-1β secretion was also investigated, but no inflammatory response was observed. Further experiments examining cytokine expression at the RNA and protein level as well as examining a wider panel of cytokines could help elucidate the importance of choline availability in cytokine secretion.

7.6 CTL1$^{-/-}$ mouse as a model of choline deficiency

Although pharmacological inhibition and antibody occlusion provide models of choline deficiency, they have the possibility of producing off-target effects and are likely limited to *in vitro* studies. The CTL1$^{-/-}$ mouse will provide a necessary tool for studying the immunometabolic implications of choline deficiency in macrophages. Although the functional studies will need to need to be substantiated and replicated, it appears that CTL1$^{-/-}$ macrophages have substantially reduced choline uptake and incorporation into lipids (Figure 11). This goes a long way towards clarifying the role of CTL1. Subsequent studies in BMDM will need to establish how other metabolic pathways that could compensate for reduced choline metabolism are influenced by CTL1 knockout, and how CTL1 knockout influences total PC levels. Once established as a model for choline deficiency, CTL1$^{-/-}$ BMDM will provide the optimal *in vitro* model for determining the influence of choline deficiency on cytokine

production. Future studies should aim to address the potential consequence of disrupting macrophage choline uptake and subsequent choline metabolism with this model during obesity

To date, there is limited knowledge on how choline transport can influence lipid metabolism *in vivo* due to the lack of an appropriate model for its study. Currently, the most thoroughly studied model of impaired choline metabolism *in vivo* is the $PEMT^{-/-}$ mouse. Although PEMT only contributes to approximately 30% of hepatic PC, $PEMT^{-/-}$ mice show hepatic steatosis, increased accumulation of hepatic triglycerides, and decreased very-low density lipoprotein secretion in the liver (Zhao et al., 2009; Zhu et al., 2003). Although $PEMT^{-/-}$ mice have contributed to the significantly to the study of choline metabolism, studies are limited to liver and adipose tissue due to PEMT's cell specific expression. CTL1's ubiquitous expression allows for the study of choline deficiency using $CTL1^{-/-}$mice in whole-body context. On top of investigating whether the $CTL1^{-/-}$ mice recapitulate the phenotype observed in $PEMT^{-/-}$ mice, it will be interesting to see how $CTL1^{-/-}$ mice respond to metabolic stress. My research has shown that CTL1 promotes a more pro-inflammatory response in response to an acute dose of LPS (Figure 13). This raises the question whether $CTL1^{-/-}$ mice exhibit a greater degree of pro-inflammatory signaling under obsess conditions. Challenging $CTL1^{-/-}$ mice with a high-fat diet could provide valuable insights into whether CTL1 plays an important role in regulating the immunometabolic response. Another future direction to take the $CTL1^{-/-}$ mice is the study of choline metabolism in an atherogenic context. It is well established that choline deficiency protects against atherosclerosis development by decreasing hepatic VLDL secretion (Zeisel et al., 1991; Zhao et al., 2009). Of particular interest in the $CTL1^{-/-}$ mice is whether cholesterol efflux is maintained in foam cells in atherosclerotic lesions. Once it is fully validated as a model for choline deficiency, the $CTL^{-/-}$ presents many future avenues of research.

8.0 CONCLUDING REMARKS

In conclusion, this research has shed light on the reciprocal link between choline metabolism and inflammation. Macrophage polarization increased choline metabolism in macrophages, which may provide PC necessary for the packaging and secretion of cytokines. This process may be mediated by CTL1, with its expression increasing following macrophage polarization. Conversely, choline deficiency altered acute cytokine secretion in response to endotoxin treatment. Although the results were variable depending on the inhibitor treatment, choline deficiency generally skewed macrophages towards a more pro-inflammatory phenotype that is associated with poorer metabolic outcomes. This study validates the importance of the interplay that exists between inflammation and metabolism and provides a viable model in the $CTL1^{-/-}$ mouse to investigate choline deficiency in an *in vivo* system.

9.0 REFERENCES

Arango Duque, G., and Descoteaux, A. (2014). Macrophage cytokines: involvement in immunity and infectious diseases. Front Immunol *5*, 491.

Asehnoune, K., Strassheim, D., Mitra, S., Yeol Kim, J., and Abraham, E. (2005). Involvement of PKCalpha/beta in TLR4 and TLR2 dependent activation of NF-kappaB. Cell Signal *17*, 385-394.

Beckmann, J., Schubert, J., Morhenn, H.G., Grau, V., Schnettler, R., and Lips, K.S. (2015). Expression of choline and acetylcholine transporters in synovial tissue and cartilage of patients with rheumatoid arthritis and osteoarthritis. Cell Tissue Res *359*, 465-477.

Best, C.H., and Huntsman, M.E. (1932). The effects of the components of lecithine upon deposition of fat in the liver. J Physiol *75*, 405-412.

Best, C.H., and Huntsman, M.E. (1935). The effect of choline on the liver fat of rats in various states of nutrition. J Physiol *83*, 255-274.

Bianchi, M.E. (2007). DAMPs, PAMPs and alarmins: all we need to know about danger. J Leukoc Biol *81*, 1-5.

Bligh, E.G., and Dyer, W.J. (1959). A rapid method of total lipid extraction and purification. Can J Biochem Physiol *37*, 911-917.

Buchman, A.L., Dubin, M.D., Moukarzel, A.A., Jenden, D.J., Roch, M., Rice, K.M., Gornbein, J., and Ament, M.E. (1995). Choline deficiency: a cause of hepatic steatosis during parenteral nutrition that can be reversed with intravenous choline supplementation. Hepatology *22*, 1399-1403.

Buroni, F.E., Pasi, F., Persico, M.G., Lodola, L., Aprile, C., and Nano, R. (2015). Evidence of 18F-FCH Uptake in Human T98G Glioblastoma Cells. Anticancer Res *35*, 6439-6443.

Cani, P.D., Amar, J., Iglesias, M.A., Poggi, M., Knauf, C., Bastelica, D., Neyrinck, A.M., Fava, F., Tuohy, K.M., Chabo, C., *et al.* (2007). Metabolic endotoxemia initiates obesity and insulin resistance. Diabetes *56*, 1761-1772.

Castoldi, A., Naffah de Souza, C., Camara, N.O., and Moraes-Vieira, P.M. (2015). The Macrophage Switch in Obesity Development. Front Immunol *6*, 637.

Caviglia, J.M., De Gomez Dumm, I.N., Coleman, R.A., and Igal, R.A. (2004). Phosphatidylcholine deficiency upregulates enzymes of triacylglycerol metabolism in CHO cells. J Lipid Res *45*, 1500-1509.

Chang, Y.H., Ho, K.T., Lu, S.H., Huang, C.N., and Shiau, M.Y. (2012). Regulation of glucose/lipid metabolism and insulin sensitivity by interleukin-4. Int J Obes (Lond) *36*, 993-998.

Chatila, T.A. (2004). Interleukin-4 receptor signaling pathways in asthma pathogenesis. Trends Mol Med *10*, 493-499.

Chawla, A., Nguyen, K.D., and Goh, Y.P. (2011). Macrophage-mediated inflammation in metabolic disease. Nat Rev Immunol *11*, 738-749.

Che, Y.H., Yamashita, T., Higuchi, H., and Tohyama, M. (2002). Changes in mRNA for choline transporter-like protein following facial nerve transection. Brain Res Mol Brain Res *101*, 122-125.

Chitraju, C., Trotzmuller, M., Hartler, J., Wolinski, H., Thallinger, G.G., Lass, A., Zechner, R., Zimmermann, R., Kofeler, H.C., and Spener, F. (2012). Lipidomic analysis of lipid droplets from murine hepatocytes reveals distinct signatures for nutritional stress. J Lipid Res *53*, 2141-2152.

Chotipanich, C., Kunawudhi, A., Promteangtrong, C., Tungsuppawattanakit, P., Sricharunrat, T., and Wongsa, P. (2016). Diagnosis of Hepatocellular Carcinoma Using C11 Choline PET/CT: Comparison with F18 FDG, ContrastEnhanced MRI and MDCT. Asian Pac J Cancer Prev *17*, 3569-3573.

Chow, J.C., Young, D.W., Golenbock, D.T., Christ, W.J., and Gusovsky, F. (1999). Toll-like receptor-4 mediates lipopolysaccharide-induced signal transduction. J Biol Chem *274*, 10689-10692.

Christensen, B., Arbour, L., Tran, P., Leclerc, D., Sabbaghian, N., Platt, R., Gilfix, B.M., Rosenblatt, D.S., Gravel, R.A., Forbes, P., *et al.* (1999). Genetic polymorphisms in methylenetetrahydrofolate reductase and methionine synthase, folate levels in red blood cells, and risk of neural tube defects. Am J Med Genet *84*, 151-157.

Chu, A.J. (1992). Bacterial lipopolysaccharide stimulates phospholipid synthesis and phosphatidylcholine breakdown in cultured human leukemia monocytic THP-1 cells. Int J Biochem *24*, 317-323.

Cole, L.K., and Vance, D.E. (2010). A role for Sp1 in transcriptional regulation of phosphatidylethanolamine N-methyltransferase in liver and 3T3-L1 adipocytes. J Biol Chem *285*, 11880-11891.

Cole, L.K., Vance, J.E., and Vance, D.E. (2012). Phosphatidylcholine biosynthesis and lipoprotein metabolism. Biochim Biophys Acta *1821*, 754-761.

Dawaliby, R., Trubbia, C., Delporte, C., Noyon, C., Ruysschaert, J.M., Van Antwerpen, P., and Govaerts, C. (2016). Phosphatidylethanolamine Is a Key Regulator of Membrane Fluidity in Eukaryotic Cells. J Biol Chem *291*, 3658-3667.

Esko, J.D., Nishijima, M., and Raetz, C.R. (1982). Animal cells dependent on exogenous phosphatidylcholine for membrane biogenesis. Proc Natl Acad Sci U S A *79*, 1698-1702.

Fagone, P., Sriburi, R., Ward-Chapman, C., Frank, M., Wang, J., Gunter, C., Brewer, J.W., and Jackowski, S. (2007). Phospholipid biosynthesis program underlying membrane expansion during B-lymphocyte differentiation. J Biol Chem *282*, 7591-7605.

Ferguson, S.M., Bazalakova, M., Savchenko, V., Tapia, J.C., Wright, J., and Blakely, R.D. (2004). Lethal impairment of cholinergic neurotransmission in hemicholinium-3-sensitive choline transporter knockout mice. Proc Natl Acad Sci U S A *101*, 8762-8767.

Finkelstein, J.D., Martin, J.J., Harris, B.J., and Kyle, W.E. (1983). Regulation of hepatic betaine-homocysteine methyltransferase by dietary betaine. J Nutr *113*, 519-521.

Fisher, M.C., Zeisel, S.H., Mar, M.H., and Sadler, T.W. (2001). Inhibitors of choline uptake and metabolism cause developmental abnormalities in neurulating mouse embryos. Teratology *64*, 114-122.

Fitzgerald, K.A., McWhirter, S.M., Faia, K.L., Rowe, D.C., Latz, E., Golenbock, D.T., Coyle, A.J., Liao, S.M., and Maniatis, T. (2003). IKKepsilon and TBK1 are essential components of the IRF3 signaling pathway. Nat Immunol *4*, 491-496.

Flesch, B.K., Wesche, J., Berthold, T., Goldmann, T., Hundt, M., Greinacher, A., and Bux, J. (2013). Expression of the CTL2 transcript variants in human peripheral blood cells and human tissues. Transfusion *53*, 3217-3223.

Friedrich, A., George, R.L., Bridges, C.C., Prasad, P.D., and Ganapathy, V. (2001). Transport of choline and its relationship to the expression of the organic cation transporters in a rat brain microvessel endothelial cell line (RBE4). Biochim Biophys Acta *1512*, 299-307.

Frohlich, J., McLeod, R., and Hon, K. (1982). Lecithin: cholesterol acyl transferase (LCAT). Clin Biochem *15*, 269-278.

Fujita, T., Shimada, A., Okada, N., and Yamamoto, A. (2006). Functional characterization of Na+-independent choline transport in primary cultures of neurons from mouse cerebral cortex. Neurosci Lett *393*, 216-221.

Fullerton, M.D., Wagner, L., Yuan, Z., and Bakovic, M. (2006). Impaired trafficking of choline transporter-like protein-1 at plasma membrane and inhibition of choline transport in THP-1 monocyte-derived macrophages. Am J Physiol Cell Physiol *290*, C1230-1238.

Gaiti, A., Brunetti, M., Woelk, H., and Porcellati, G. (1976). Relationships between base-exchange reaction and the microsomal phospholipid pool in the rat brain in vitro. Lipids *11*, 823-829.

Galvan-Pena, S., and O'Neill, L.A. (2014). Metabolic reprograming in macrophage polarization. Front Immunol *5*, 420.

Gao, Z., Hwang, D., Bataille, F., Lefevre, M., York, D., Quon, M.J., and Ye, J. (2002). Serine phosphorylation of insulin receptor substrate 1 by inhibitor kappa B kinase complex. J Biol Chem *277*, 48115-48121.

Giovannini, E., Lazzeri, P., Milano, A., Gaeta, M.C., and Ciarmiello, A. (2015). Clinical applications of choline PET/CT in brain tumors. Curr Pharm Des *21*, 121-127.

Glunde, K., Bhujwalla, Z.M., and Ronen, S.M. (2011). Choline metabolism in malignant transformation. Nat Rev Cancer *11*, 835-848.

Gorboulev, V., Ulzheimer, J.C., Akhoundova, A., Ulzheimer-Teuber, I., Karbach, U., Quester, S., Baumann, C., Lang, F., Busch, A.E., and Koepsell, H. (1997). Cloning and characterization of two human polyspecific organic cation transporters. DNA Cell Biol *16*, 871-881.

Gordon, S. (2003). Alternative activation of macrophages. Nat Rev Immunol *3*, 23-35.

Gordon, S., and Taylor, P.R. (2005). Monocyte and macrophage heterogeneity. Nat Rev Immunol *5*, 953-964.

Grove, R.I., Allegretto, N.J., Kiener, P.A., and Warr, G.A. (1990). Lipopolysaccharide (LPS) alters phosphatidylcholine metabolism in elicited peritoneal macrophages. J Leukoc Biol *48*, 38-42.

Haga, T. (2014). Molecular properties of the high-affinity choline transporter CHT1. J Biochem *156*, 181-194.

Henneberry, A.L., Wright, M.M., and McMaster, C.R. (2002). The major sites of cellular phospholipid synthesis and molecular determinants of Fatty Acid and lipid head group specificity. Mol Biol Cell *13*, 3148-3161.

Hershey, J.M., and Soskin, S. (1931). Substitution of "lecithin" for raw pancreas in the diet of the depancreatized dog. Am J Physiol *98*, 74-85.

Hotamisligil, G.S., Shargill, N.S., and Spiegelman, B.M. (1993). Adipose expression of tumor necrosis factor-alpha: direct role in obesity-linked insulin resistance. Science *259*, 87-91.

Hou, J., Schindler, U., Henzel, W.J., Ho, T.C., Brasseur, M., and McKnight, S.L. (1994). An interleukin-4-induced transcription factor: IL-4 Stat. Science *265*, 1701-1706.

Howell, K.W., Meng, X., Fullerton, D.A., Jin, C., Reece, T.B., and Cleveland, J.C., Jr. (2011). Toll-like receptor 4 mediates oxidized LDL-induced macrophage differentiation to foam cells. J Surg Res *171*, e27-31.

Inazu, M. (2014). Choline transporter-like proteins CTLs/SLC44 family as a novel molecular target for cancer therapy. Biopharm Drug Dispos *35*, 431-449.

Inazu, M., Takeda, H., and Matsumiya, T. (2005). Molecular and functional characterization of an Na+-independent choline transporter in rat astrocytes. J Neurochem *94*, 1427-1437.

Iorio, E., Ricci, A., Bagnoli, M., Pisanu, M.E., Castellano, G., Di Vito, M., Venturini, E., Glunde, K., Bhujwalla, Z.M., Mezzanzanica, D., *et al.* (2010). Activation of phosphatidylcholine cycle enzymes in human epithelial ovarian cancer cells. Cancer Res *70*, 2126-2135.

Ishiguro, N., Oyabu, M., Sato, T., Maeda, T., Minami, H., and Tamai, I. (2008). Decreased biosynthesis of lung surfactant constituent phosphatidylcholine due to inhibition of choline transporter by gefitinib in lung alveolar cells. Pharm Res *25*, 417-427.

Italiani, P., and Boraschi, D. (2014). From Monocytes to M1/M2 Macrophages: Phenotypical vs. Functional Differentiation. Front Immunol *5*, 514.

Jackowski, S., Wang, J., and Baburina, I. (2000). Activity of the phosphatidylcholine biosynthetic pathway modulates the distribution of fatty acids into glycerolipids in proliferating cells. Biochim Biophys Acta *1483*, 301-315.

Jellinek, M., Strength, D.R., and Thayer, S.A. (1959). Isolation and identification of the products of the oxidation of choline. J Biol Chem *234*, 1171-1173.

Kang, K., Reilly, S.M., Karabacak, V., Gangl, M.R., Fitzgerald, K., Hatano, B., and Lee, C.H. (2008). Adipocyte-derived Th2 cytokines and myeloid PPARdelta regulate macrophage polarization and insulin sensitivity. Cell Metab *7*, 485-495.

Kaplan, M.H., Schindler, U., Smiley, S.T., and Grusby, M.J. (1996). Stat6 is required for mediating responses to IL-4 and for development of Th2 cells. Immunity *4*, 313-319.

Karin, M., and Gallagher, E. (2009). TNFR signaling: ubiquitin-conjugated TRAFfic signals control stop-and-go for MAPK signaling complexes. Immunol Rev *228*, 225-240.

Kawasaki, T., and Kawai, T. (2014). Toll-like receptor signaling pathways. Front Immunol *5*, 461.

Kennedy, E.P., and Weiss, S.B. (1956). The function of cytidine coenzymes in the biosynthesis of phospholipides. J Biol Chem *222*, 193-214.

Kiyan, Y., Tkachuk, S., Hilfiker-Kleiner, D., Haller, H., Fuhrman, B., and Dumler, I. (2014). oxLDL induces inflammatory responses in vascular smooth muscle cells via urokinase receptor association with CD36 and TLR4. J Mol Cell Cardiol *66*, 72-82.

Kommareddi, P., Nair, T., Kakaraparthi, B.N., Galano, M.M., Miller, D., Laczkovich, I., Thomas, T., Lu, L., Rule, K., Kabara, L., *et al.* (2015). Hair Cell Loss, Spiral Ganglion Degeneration, and Progressive Sensorineural Hearing Loss in Mice with Targeted Deletion of Slc44a2/Ctl2. J Assoc Res Otolaryngol *16*, 695-712.

Kommareddi, P.K., Nair, T.S., Vallurupalli, M., Telian, S.A., Arts, H.A., El-Kashlan, H.K., Sataloff, R.T., and Carey, T.E. (2009). Autoantibodies to recombinant human CTL2 in autoimmune hearing loss. Laryngoscope *119*, 924-932.

Kondo, M., Takeshita, T., Ishii, N., Nakamura, M., Watanabe, S., Arai, K., and Sugamura, K. (1993). Sharing of the interleukin-2 (IL-2) receptor gamma chain between receptors for IL-2 and IL-4. Science *262*, 1874-1877.

Krahmer, N., Guo, Y., Wilfling, F., Hilger, M., Lingrell, S., Heger, K., Newman, H.W., Schmidt-Supprian, M., Vance, D.E., Mann, M., *et al.* (2011). Phosphatidylcholine synthesis for lipid droplet expansion is mediated by localized activation of CTP:phosphocholine cytidylyltransferase. Cell Metab *14*, 504-515.

Li, Z., Agellon, L.B., Allen, T.M., Umeda, M., Jewell, L., Mason, A., and Vance, D.E. (2006). The ratio of phosphatidylcholine to phosphatidylethanolamine influences membrane integrity and steatohepatitis. Cell Metab *3*, 321-331.

Lin, S.C., Lo, Y.C., and Wu, H. (2010). Helical assembly in the MyD88-IRAK4-IRAK2 complex in TLR/IL-1R signalling. Nature *465*, 885-890.

Linkous, A., and Yazlovitskaya, E. (2010). Cytosolic phospholipase A2 as a mediator of disease pathogenesis. Cell Microbiol *12*, 1369-1377.

Livak, K.J., and Schmittgen, T.D. (2001). Analysis of relative gene expression data using real-time quantitative PCR and the 2(-Delta Delta C(T)) Method. Methods *25*, 402-408.

Lumeng, C.N., Bodzin, J.L., and Saltiel, A.R. (2007). Obesity induces a phenotypic switch in adipose tissue macrophage polarization. J Clin Invest *117*, 175-184.

Lykidis, A., Baburina, I., and Jackowski, S. (1999). Distribution of CTP:phosphocholine cytidylyltransferase (CCT) isoforms. Identification of a new CCTbeta splice variant. J Biol Chem *274*, 26992-27001.

Machova, E., O'Regan, S., Newcombe, J., Meunier, F.M., Prentice, J., Dove, R., Lisa, V., and Dolezal, V. (2009). Detection of choline transporter-like 1 protein CTL1 in neuroblastoma x glioma cells and in the CNS, and its role in choline uptake. J Neurochem *110*, 1297-1309.

Malabarba, M.G., Kirken, R.A., Rui, H., Koettnitz, K., Kawamura, M., O'Shea, J.J., Kalthoff, F.S., and Farrar, W.L. (1995). Activation of JAK3, but not JAK1, is critical to interleukin-4 (IL4) stimulated proliferation and requires a membrane-proximal region of IL4 receptor alpha. J Biol Chem *270*, 9630-9637.

Manderson, A.P., Kay, J.G., Hammond, L.A., Brown, D.L., and Stow, J.L. (2007). Subcompartments of the macrophage recycling endosome direct the differential secretion of IL-6 and TNFalpha. J Cell Biol *178*, 57-69.

Marchbanks, R.M., and Kessler, P.D. (1982). The independency of choline transport and acetylcholine synthesis. J Neurochem *39*, 1424-1433.

Marciniak, S.J., Yun, C.Y., Oyadomari, S., Novoa, I., Zhang, Y., Jungreis, R., Nagata, K., Harding, H.P., and Ron, D. (2004). CHOP induces death by promoting protein synthesis and oxidation in the stressed endoplasmic reticulum. Genes Dev *18*, 3066-3077.

McNelis, J.C., and Olefsky, J.M. (2014). Macrophages, immunity, and metabolic disease. Immunity *41*, 36-48.

Mercurio, F., Zhu, H., Murray, B.W., Shevchenko, A., Bennett, B.L., Li, J., Young, D.B., Barbosa, M., Mann, M., Manning, A., *et al.* (1997). IKK-1 and IKK-2: cytokine-activated IkappaB kinases essential for NF-kappaB activation. Science *278*, 860-866.

Michel, V., and Bakovic, M. (2009). The solute carrier 44A1 is a mitochondrial protein and mediates choline transport. FASEB J *23*, 2749-2758.

Michel, V., Yuan, Z., Ramsubir, S., and Bakovic, M. (2006). Choline transport for phospholipid synthesis. Exp Biol Med (Maywood) *231*, 490-504.

Moessinger, C., Klizaite, K., Steinhagen, A., Philippou-Massier, J., Shevchenko, A., Hoch, M., Ejsing, C.S., and Thiele, C. (2014). Two different pathways of phosphatidylcholine synthesis, the Kennedy Pathway and the Lands Cycle, differentially regulate cellular triacylglycerol storage. BMC Cell Biol *15*, 43.

Murray, R.Z., and Stow, J.L. (2014). Cytokine Secretion in Macrophages: SNAREs, Rabs, and Membrane Trafficking. Front Immunol *5*, 538.

Nair, T.S., Kozma, K.E., Hoefling, N.L., Kommareddi, P.K., Ueda, Y., Gong, T.W., Lomax, M.I., Lansford, C.D., Telian, S.A., Satar, B., *et al.* (2004). Identification and characterization of choline transporter-like protein 2, an inner ear glycoprotein of 68 and 72 kDa that is the target of antibody-induced hearing loss. J Neurosci *24*, 1772-1779.

Nelms, K., Keegan, A.D., Zamorano, J., Ryan, J.J., and Paul, W.E. (1999). The IL-4 receptor: signaling mechanisms and biologic functions. Annu Rev Immunol *17*, 701-738.

Nishitoh, H. (2012). CHOP is a multifunctional transcription factor in the ER stress response. J Biochem *151*, 217-219.

Nishiyama, R., Nagashima, F., Iwao, B., Kawai, Y., Inoue, K., Midori, A., Yamanaka, T., Uchino, H., and Inazu, M. (2016). Identification and functional analysis of choline transporter in tongue cancer: A novel molecular target for tongue cancer therapy. J Pharmacol Sci *131*, 101-109.

O'Regan, S., Traiffort, E., Ruat, M., Cha, N., Compaore, D., and Meunier, F.M. (2000). An electric lobe suppressor for a yeast choline transport mutation belongs to a new family of transporter-like proteins. Proc Natl Acad Sci U S A *97*, 1835-1840.

Oakes, S.A., Candotti, F., Johnston, J.A., Chen, Y.Q., Ryan, J.J., Taylor, N., Liu, X., Hennighausen, L., Notarangelo, L.D., Paul, W.E., *et al.* (1996). Signaling via IL-2 and IL-4 in JAK3-deficient severe combined immunodeficiency lymphocytes: JAK3-dependent and independent pathways. Immunity *5*, 605-615.

Obeid, R. (2013). The metabolic burden of methyl donor deficiency with focus on the betaine homocysteine methyltransferase pathway. Nutrients *5*, 3481-3495.

Oda, Y. (1999). Choline acetyltransferase: the structure, distribution and pathologic changes in the central nervous system. Pathol Int *49*, 921-937.

Odegaard, J.I., and Chawla, A. (2011). Alternative macrophage activation and metabolism. Annu Rev Pathol *6*, 275-297.

Okuda, T., Haga, T., Kanai, Y., Endou, H., Ishihara, T., and Katsura, I. (2000). Identification and characterization of the high-affinity choline transporter. Nat Neurosci *3*, 120-125.

Orr, J.S., Puglisi, M.J., Ellacott, K.L., Lumeng, C.N., Wasserman, D.H., and Hasty, A.H. (2012). Toll-like receptor 4 deficiency promotes the alternative activation of adipose tissue macrophages. Diabetes *61*, 2718-2727.

Pelis, R.M., and Wright, S.H. (2014). SLC22, SLC44, and SLC47 transporters--organic anion and cation transporters: molecular and cellular properties. Curr Top Membr *73*, 233-261.

Peyssonnaux, C., Datta, V., Cramer, T., Doedens, A., Theodorakis, E.A., Gallo, R.L., Hurtado-Ziola, N., Nizet, V., and Johnson, R.S. (2005). HIF-1alpha expression regulates the bactericidal capacity of phagocytes. J Clin Invest *115*, 1806-1815.

Pogribny, I.P., Basnakian, A.G., Miller, B.J., Lopatina, N.G., Poirier, L.A., and James, S.J. (1995). Breaks in genomic DNA and within the p53 gene are associated with hypomethylation in livers of folate/methyl-deficient rats. Cancer Res *55*, 1894-1901.

Poltorak, A., He, X., Smirnova, I., Liu, M.Y., Van Huffel, C., Du, X., Birdwell, D., Alejos, E., Silva, M., Galanos, C., *et al.* (1998). Defective LPS signaling in C3H/HeJ and C57BL/10ScCr mice: mutations in Tlr4 gene. Science *282*, 2085-2088.

Post, M., Batenburg, J.J., Schuurmans, E.A., and Van Golde, L.M. (1982). The rate-limiting step in the biosynthesis of phosphatidylcholine by alveolar type II cells from adult rat lung. Biochim Biophys Acta *712*, 390-394.

Reske, S.N., Blumstein, N.M., Neumaier, B., Gottfried, H.W., Finsterbusch, F., Kocot, D., Moller, P., Glatting, G., and Perner, S. (2006). Imaging prostate cancer with 11C-choline PET/CT. J Nucl Med *47*, 1249-1254.

Rodriguez-Prados, J.C., Traves, P.G., Cuenca, J., Rico, D., Aragones, J., Martin-Sanz, P., Cascante, M., and Bosca, L. (2010). Substrate fate in activated macrophages: a comparison between innate, classic, and alternative activation. J Immunol *185*, 605-614.

Ryan, J.J., McReynolds, L.J., Huang, H., Nelms, K., and Paul, W.E. (1998). Characterization of a mobile Stat6 activation motif in the human IL-4 receptor. J Immunol *161*, 1811-1821.

Schutze, S., Potthoff, K., Machleidt, T., Berkovic, D., Wiegmann, K., and Kronke, M. (1992). TNF activates NF-kappa B by phosphatidylcholine-specific phospholipase C-induced "acidic" sphingomyelin breakdown. Cell *71*, 765-776.

Shi, H., Kokoeva, M.V., Inouye, K., Tzameli, I., Yin, H., and Flier, J.S. (2006). TLR4 links innate immunity and fatty acid-induced insulin resistance. J Clin Invest *116*, 3015-3025.

Sweet, D.H., Miller, D.S., and Pritchard, J.B. (2001). Ventricular choline transport: a role for organic cation transporter 2 expressed in choroid plexus. J Biol Chem *276*, 41611-41619.

Takaesu, G., Surabhi, R.M., Park, K.J., Ninomiya-Tsuji, J., Matsumoto, K., and Gaynor, R.B. (2003). TAK1 is critical for IkappaB kinase-mediated activation of the NF-kappaB pathway. J Mol Biol *326*, 105-115.

Taniguchi, M., and Okazaki, T. (2014). The role of sphingomyelin and sphingomyelin synthases in cell death, proliferation and migration-from cell and animal models to human disorders. Biochim Biophys Acta *1841*, 692-703.

Testerink, N., van der Sanden, M.H., Houweling, M., Helms, J.B., and Vaandrager, A.B. (2009). Depletion of phosphatidylcholine affects endoplasmic reticulum morphology and protein traffic at the Golgi complex. J Lipid Res *50*, 2182-2192.

Tian, Y., Pate, C., Andreolotti, A., Wang, L., Tuomanen, E., Boyd, K., Claro, E., and Jackowski, S. (2008). Cytokine secretion requires phosphatidylcholine synthesis. J Cell Biol *181*, 945-957.

Traiffort, E., O'Regan, S., and Ruat, M. (2013). The choline transporter-like family SLC44: properties and roles in human diseases. Mol Aspects Med *34*, 646-654.

Tsao, C.H., Shiau, M.Y., Chuang, P.H., Chang, Y.H., and Hwang, J. (2014). Interleukin-4 regulates lipid metabolism by inhibiting adipogenesis and promoting lipolysis. J Lipid Res *55*, 385-397.

Ueki, K., Kondo, T., and Kahn, C.R. (2004). Suppressor of cytokine signaling 1 (SOCS-1) and SOCS-3 cause insulin resistance through inhibition of tyrosine phosphorylation of insulin receptor substrate proteins by discrete mechanisms. Mol Cell Biol *24*, 5434-5446.

Ueland, P.M. (2011). Choline and betaine in health and disease. J Inherit Metab Dis *34*, 3-15.
van der Sanden, M.H., Houweling, M., van Golde, L.M., and Vaandrager, A.B. (2003). Inhibition of phosphatidylcholine synthesis induces expression of the endoplasmic reticulum

stress and apoptosis-related protein CCAAT/enhancer-binding protein-homologous protein (CHOP/GADD153). Biochem J *369*, 643-650.

Vance, D.E., Walkey, C.J., and Cui, Z. (1997). Phosphatidylethanolamine N-methyltransferase from liver. Biochim Biophys Acta *1348*, 142-150.

Vats, D., Mukundan, L., Odegaard, J.I., Zhang, L., Smith, K.L., Morel, C.R., Wagner, R.A., Greaves, D.R., Murray, P.J., and Chawla, A. (2006). Oxidative metabolism and PGC-1beta attenuate macrophage-mediated inflammation. Cell Metab *4*, 13-24.

Wang, L.M., Myers, M.G., Jr., Sun, X.J., Aaronson, S.A., White, M., and Pierce, J.H. (1993). IRS-1: essential for insulin- and IL-4-stimulated mitogenesis in hematopoietic cells. Science *261*, 1591-1594.

Weisberg, S.P., McCann, D., Desai, M., Rosenbaum, M., Leibel, R.L., and Ferrante, A.W., Jr. (2003). Obesity is associated with macrophage accumulation in adipose tissue. J Clin Invest *112*, 1796-1808.

Wille, S., Szekeres, A., Majdic, O., Prager, E., Staffler, G., Stockl, J., Kunthalert, D., Prieschl, E.E., Baumruker, T., Burtscher, H., *et al.* (2001). Characterization of CDw92 as a member of the choline transporter-like protein family regulated specifically on dendritic cells. J Immunol *167*, 5795-5804.

Wurster, A.L., Withers, D.J., Uchida, T., White, M.F., and Grusby, M.J. (2002). Stat6 and IRS-2 cooperate in interleukin 4 (IL-4)-induced proliferation and differentiation but are dispensable for IL-4-dependent rescue from apoptosis. Mol Cell Biol *22*, 117-126.

Yamamoto, M., Sato, S., Hemmi, H., Hoshino, K., Kaisho, T., Sanjo, H., Takeuchi, O., Sugiyama, M., Okabe, M., Takeda, K., *et al.* (2003). Role of adaptor TRIF in the MyD88-independent toll-like receptor signaling pathway. Science *301*, 640-643.

Yamazaki, K., Gohda, J., Kanayama, A., Miyamoto, Y., Sakurai, H., Yamamoto, M., Akira, S., Hayashi, H., Su, B., and Inoue, J. (2009). Two mechanistically and temporally distinct NF-kappaB activation pathways in IL-1 signaling. Sci Signal *2*, ra66.

Ye, H., Arron, J.R., Lamothe, B., Cirilli, M., Kobayashi, T., Shevde, N.K., Segal, D., Dzivenu, O.K., Vologodskaia, M., Yim, M., *et al.* (2002). Distinct molecular mechanism for initiating TRAF6 signalling. Nature *418*, 443-447.

Yen, C.L., Mar, M.H., and Zeisel, S.H. (1999). Choline deficiency-induced apoptosis in PC12 cells is associated with diminished membrane phosphatidylcholine and sphingomyelin, accumulation of ceramide and diacylglycerol, and activation of a caspase. FASEB J *13*, 135-142.

Young, M.M., Kester, M., and Wang, H.G. (2013). Sphingolipids: regulators of crosstalk between apoptosis and autophagy. J Lipid Res *54*, 5-19.

Yuan, Z., Tie, A., Tarnopolsky, M., and Bakovic, M. (2006). Genomic organization, promoter activity, and expression of the human choline transporter-like protein 1. Physiol Genomics *26*, 76-90.

Yuan, Z., Wagner, L., Poloumienko, A., and Bakovic, M. (2004). Identification and expression of a mouse muscle-specific CTL1 gene. Gene *341*, 305-312.

Zeisel, S.H. (2012). A brief history of choline. Ann Nutr Metab *61*, 254-258.

Zeisel, S.H., Da Costa, K.A., Franklin, P.D., Alexander, E.A., Lamont, J.T., Sheard, N.F., and Beiser, A. (1991). Choline, an essential nutrient for humans. FASEB J *5*, 2093-2098.

Zhao, Y., Su, B., Jacobs, R.L., Kennedy, B., Francis, G.A., Waddington, E., Brosnan, J.T., Vance, J.E., and Vance, D.E. (2009). Lack of phosphatidylethanolamine N-methyltransferase alters plasma VLDL phospholipids and attenuates atherosclerosis in mice. Arterioscler Thromb Vasc Biol *29*, 1349-1355.

Zhou, X., Yang, W., and Li, J. (2006). Ca2+- and protein kinase C-dependent signaling pathway for nuclear factor-kappaB activation, inducible nitric-oxide synthase expression, and tumor necrosis factor-alpha production in lipopolysaccharide-stimulated rat peritoneal macrophages. J Biol Chem *281*, 31337-31347.

Zhu, X., Song, J., Mar, M.H., Edwards, L.J., and Zeisel, S.H. (2003). Phosphatidylethanolamine N-methyltransferase (PEMT) knockout mice have hepatic steatosis and abnormal hepatic choline metabolite concentrations despite ingesting a recommended dietary intake of choline. Biochem J *370*, 987-993.

10.0 CONTRIBUTIONS OF COLLABORATORS

Figure 10 was adapted from a figure constructed by Rebecca Yaworski.

Kaitlyn Margison produced the Western blot image for CTL1 expression seen in Figure 9 and helped to conduct the experiments outlined for objective #2. Her help was much appreciated.

11.0 APPENDIX

Supplementary Figure 1. Acetylcholine synthesis in cholinergic neurons

ChAT – choline acetyltransferase

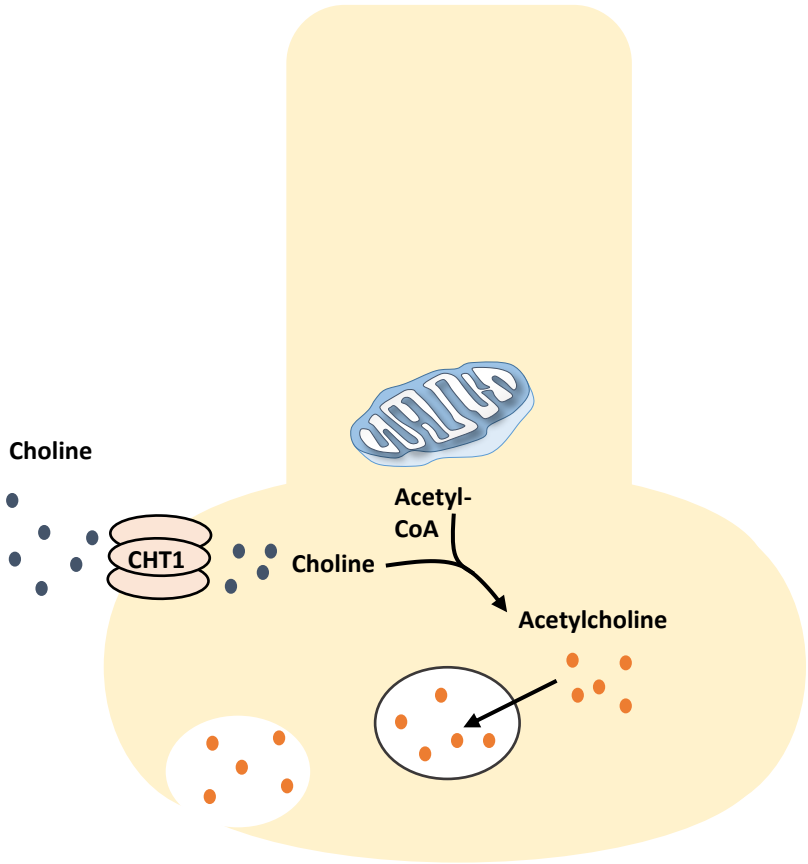
Choline
CHT1
Choline
Acetyl-
CoA
Acetylcholine

Supplementary Figure 2. Mitochondrial betaine synthesis in the liver and kidney.

BHMT – betaine-homocysteine-S-methyltransferase; SAM – S-adenosylmethionine; SAH – S-adenosylhomocysteine; DMG - dimethylglycine

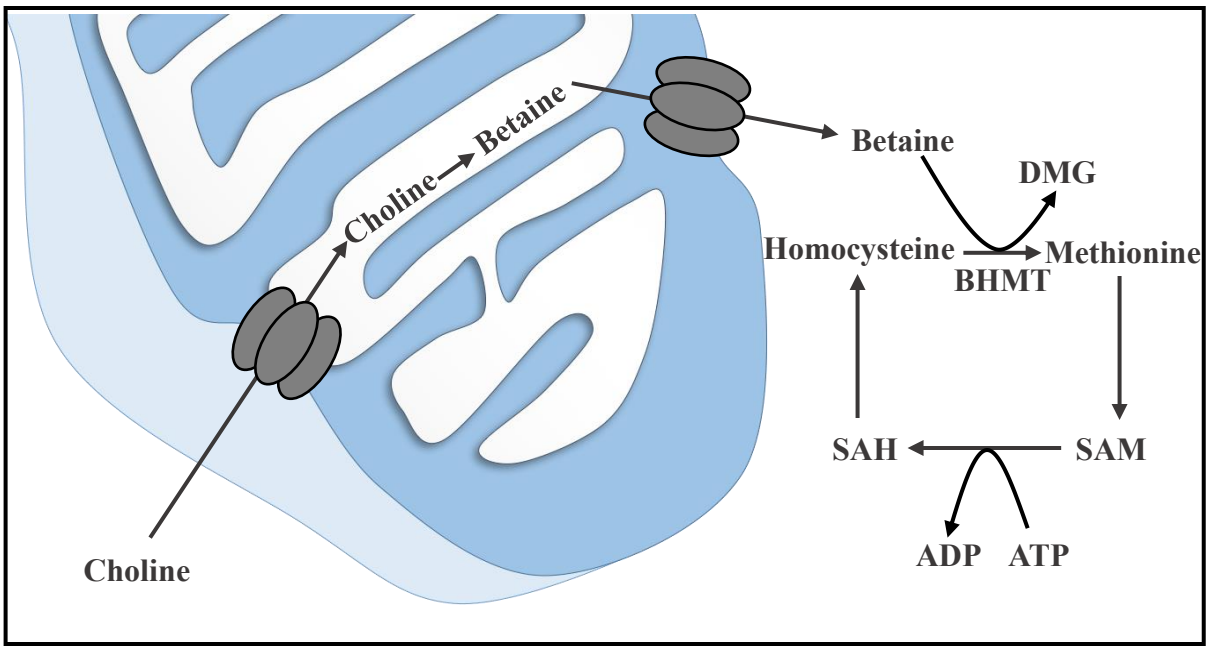
Choline → Betaine
Betaine
DMG
Homocysteine
Methionine
BHMT
SAH
SAM
ADP
ATP
Choline

Supplementary Figure 3. Classical activation through TLR4

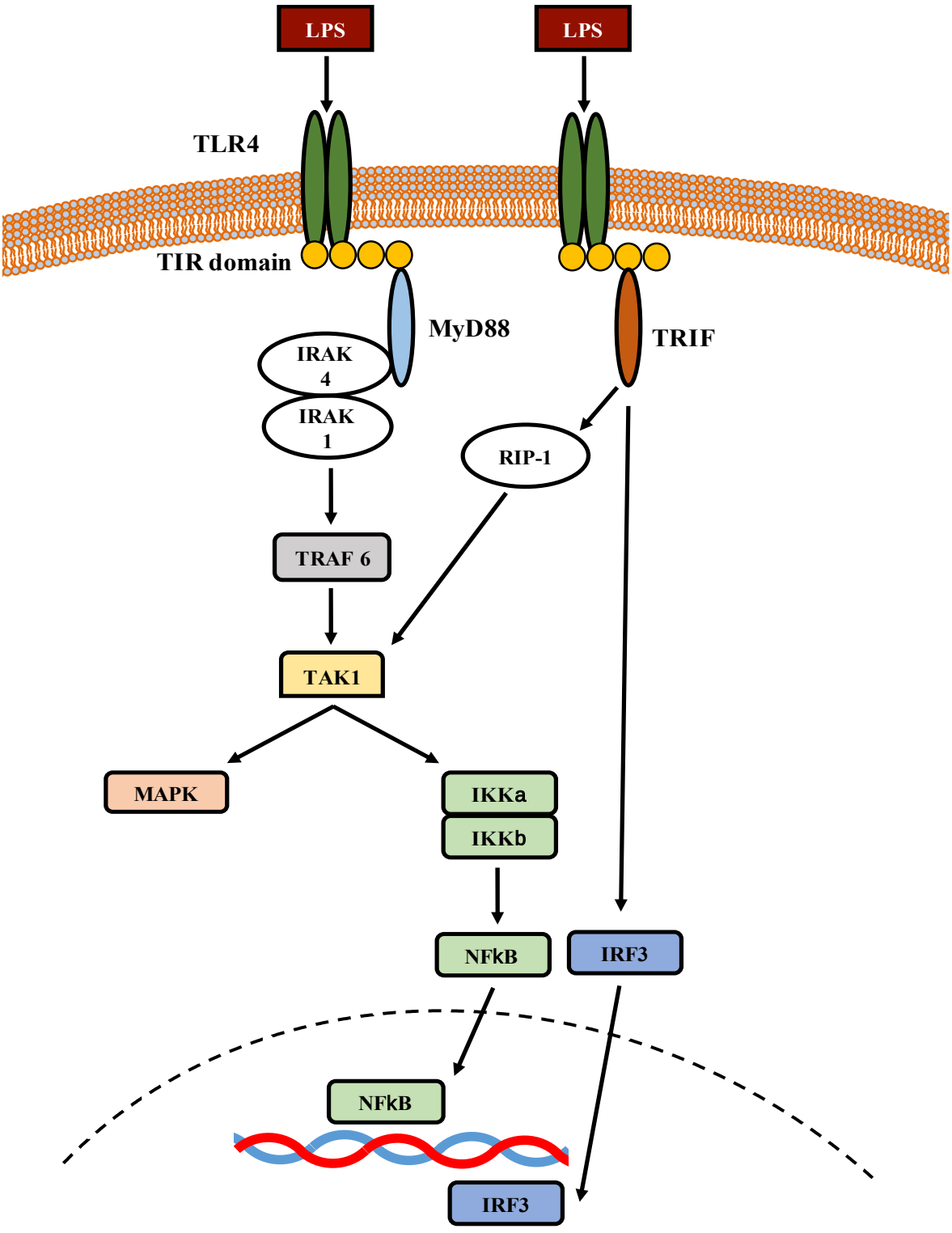
LPS
LPS
TLR4
TIR domain
MyD88
TRIF
IRAK 4
IRAK 1
RIP-1
TRAF 6
TAK1
MAPK
IKKa
IKKb
NFkB
IRF3
NFkB
IRF3

Supplementary Figure 4. Alternative activation through the JAK/STAT pathway.

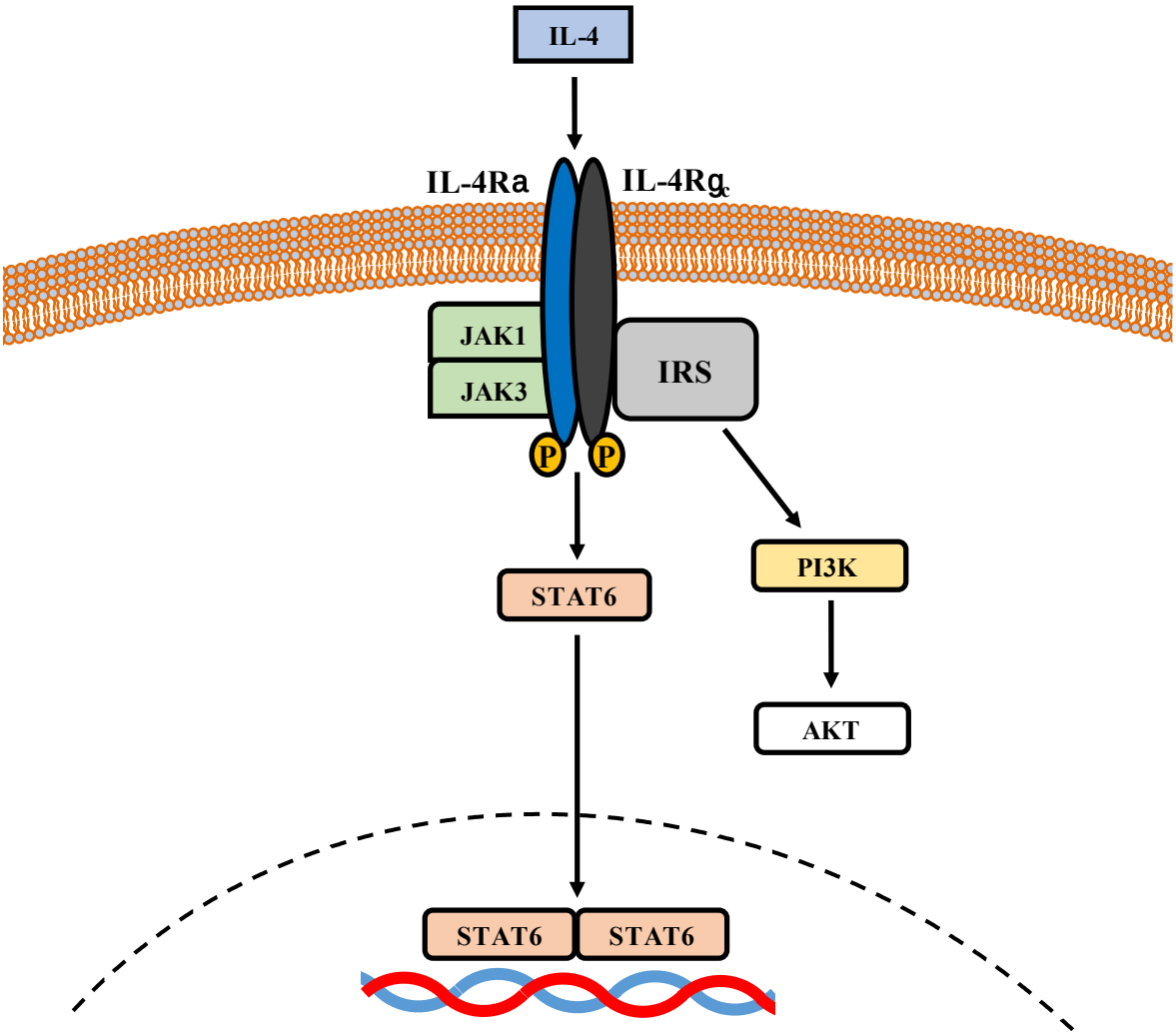
IL-4
IL-4Ra
IL-4Rgc
JAK1
JAK3
IRS
P
P
STAT6
PI3K
AKT
STAT6
STAT6

Supplementary Figure 5. Primers for CTL1$^{-/-}$ genotyping

When PCR is run with primers 10 and 12, the size of the band indicates the presence of a floxed or wild-type CTL1 allele. Polymerization with primers 11 and 17 indicates exon 3 of CTL1 has been knocked out.

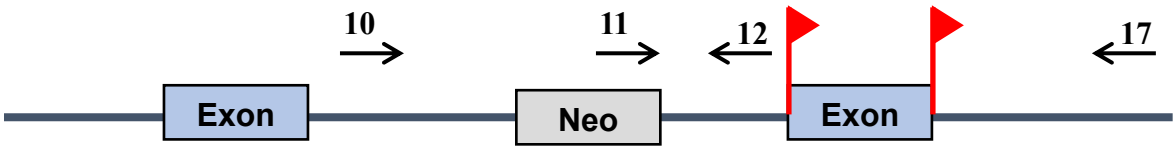

Primer	Sequence
10	TAC TGT GAC CAG CCC CTG TCT GAG
11	AGC GCA TCG CCT TCT ATC GCC TTC
12	TTC AAC AGC AGC AGT CAC CAC TTG
17	AGG ACA ATT AAG GTC AGG AGT TTC

Supplementary Figure 6. Effect of classical activation on choline uptake in RAW 264.7 macrophages.

Rate of choline uptake (A), kinetics of choline uptake (B), and HC-3 IC_{50} (C) experiments were conducted in the same manner as the BMDM experiments, which are described in detail in the methods.

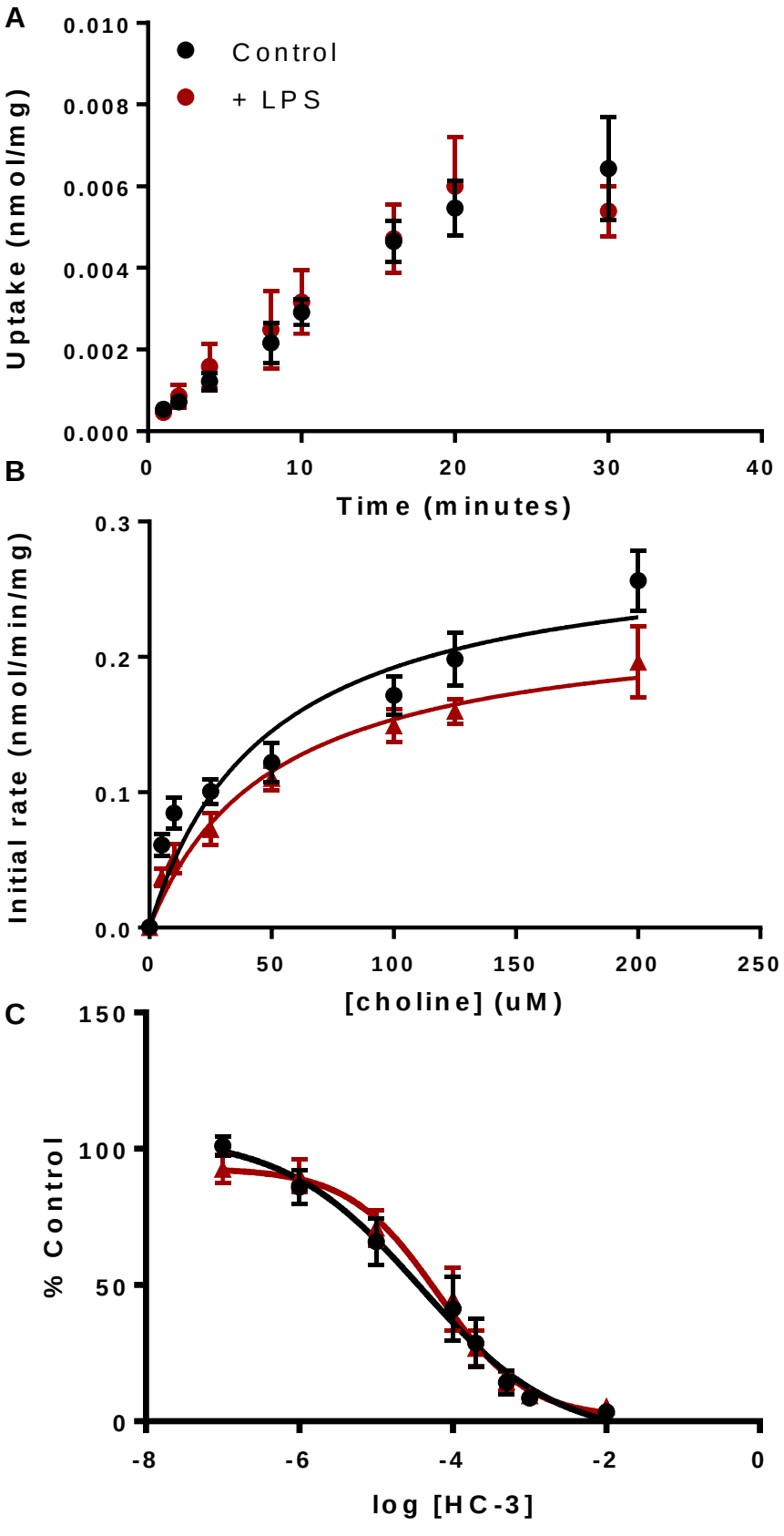
A
0.010
0.008
0.006
0.004
0.002
0.000
Uptake (nmol/mg)
Control
+ LPS
0
10
20
30
40
Time (minutes)
B
0.3
0.2
0.1
0.0
Initial rate (nmol/min/mg)
0
50
100
150
200
250
[choline] (uM)
C
150
100
50
0
% Control
-8
-6
-4
-2
0
log [HC-3]

Supplementary Table 1. List RT-PCR primers

Gene	TaqMan Primer
TNF α	Mm00443258_m1
TGF β	Mm01178820_m1
iNOS	Mm00440502_m1
Arginase	Mm00475988_m1
IL-6	Mm00446190_m1
IL-1β	Mm00434228_m1
β- actin	Mm00607939_s1
CD 206	Mm00485148_m1
TATA binding protein	Mm00446973_m1
CTL1	Mm01350815_m1
CTL2	Mm00507664_m1
CTL3	Mm000520420_m1
CTL4	Mm00469893_m1
CTL5	Mm01317372_m1
OCT1	Mm00456303_m1
OCT2	Mm00457295_m1
OCT 3	Mm00488294_m1
OCT 4	Mm00436615_m1
CHT 1	Mm00452075_m1